Characterisation and modelling of praseodymium-doped fibre amplifiers

van de Sluis, H.J.D.

Award date:
2001

Eindhoven University of Technology
Faculty of Electrical Engineering
Division of Telecommunication Technology and Electromagnetics
Electro-Optical Communication Group

Characterisation and Modelling of Praseodymium-doped Fibre Amplifiers

By H.J.D. van de Sluis

Master of Science Thesis
August 2001

Supervisors:
Dr.ir. H. de Waardt
Ir. R.C. Schimmel

Graduation professor:
Prof.ir. G.D. Khoe

Abstract

On the project "1.3 μm Praseodymium-doped Fibre Amplifiers based on Germanium Gallium Sulfide Glasses" research is performed on an efficient optical doped-fibre amplifier based on a germanium gallium sulfide glass host doped with praseodymium. This thesis reports on the graduation work done on characterisation of a practical praseodymium-doped fibre amplifier (PDFA). The work is done for the Electro-Optical Communication group of the Telecommunications and Electromagnetism division of the faculty of Electrical Engineering of the Eindhoven University of Technology.

The amplifier is set up with commercial available praseodymium-doped fluoride fibre modules. The project is mainly focused on different amplifier configurations and amplifier applications. Possible configurations are co-, counter- and bi-directional pumped amplifiers, in reference to the signal direction. Discussed amplifier applications are preamplifier, inline amplifier and booster amplifier. Experiments are performed to characterize the amplifier behavior. These measurements were primarily focused on signal gain but also the amplifier noise performance was studied. The measurement environment has been automated because of the large quantity of required measurements. In addition, these results were used to validate an already available fibre amplifier model. The model was used to examine the influence of different fibre parameters and pumping schemes on amplifier signal gain. Additionally the model was also used to simulate the amplifier noise figure.

Finally, experiments were performed on a signal double-pass amplifier configuration. In this configuration, a Faraday rotator mirror is placed at the end of the praseodymium-doped fibre to reflect the signal back into the active fibre. An optical circulator at the input of the amplifier directs the backward propagating signal to the amplifier output port. This way the signal passes the doped fibre twice and benefits more from the available gain properties of the active fibre. This resulted in much higher small signal gain compared to a single-pass set-up.

Table of contents

List of abbreviations

APD	Avalanche Photo Diode
ASE	Amplified Spontaneous Emission
BPF	Band Pass Filter
CW	Continuous Wave
EDFA	Erbium-Doped Fibre Amplifier
ESA	Excited-State Absorption
FRM	Faraday Rotator Mirror
GSA	Ground State Absorption
IR	Infrared
MQW	Multiple Quantum Well
NA	Numerical Aperture
OSA	Optical Spectrum Analyser
OTDM	Optical Time-Domain Multiplexing
PDF	Praseodymium-Doped Fibre
PDFA	Praseodymium-Doped Fibre Amplifier
PIN	Positive-Intrinsic-Negative
PM	Power Meter
SNR	Signal-to-Noise Ratio
SOA	Semiconductor Optical Amplifier
SPM	Self-Phase Modulation
SSE	Source Spontaneous Emission
TLS	Tunable Laser Source
WDM	Wavelength Division Multiplexing
YFL	Ytterbium Fibre Laser

1 Introduction

1.1 Optical fibre telecommunications systems

Nowadays, the backbone of telecommunications networks is built up out of optical fibres. These fibres have become a medium for low loss and high-speed data transmission. The huge bandwidth of the optical fibre allows huge amounts of information to be transported over very long distances. The use of techniques as wavelength division multiplexing (WDM) and optical time-domain multiplexing (OTDM) increases the network capacity even more.

Historically, optical telecommunications systems operate in three spectral regions. In each region the attenuation spectrum of the silica optical fibre exhibits low intrinsic loss. The first region is centered at 0.85 μm, the second at 1.31 μm and the third at 1.55 μm. Although the silica fibres are of the highest purity, a telecommunications signal is still attenuated by intrinsic scattering and absorption processes. Beyond a certain transmission distance the telecommunication signal becomes too small for detection. This introduces the need for amplification of the optical signal. Initially electronic repeaters where employed for this task reshaping and amplifying the signal.

From the late eighties, optical amplifiers made a forceful emergence, which in the beginning had taken the form of a semiconductor optical amplifier (SOA). These were followed by laser-diode-pumped erbium-doped fibres. Large systems spanning continental and intercontinental distances no longer have to rely merely upon the use of electronic repeaters. Some advantages of practical optical amplifiers are that they offer a much wider operating bandwidth, can amplify signals at different wavelength simultaneously, are bit transparent and insensitive to the type of signal modulation in contrast to the electronic repeaters used so far in optical communications.

1.2 Rare earth-doped fibre amplifiers

The bases for fibre amplifiers are materials that can produce optical gain by a stimulated emission process. By doping a fibre with a rare earth ion, amplification of the signal can be achieved. From the ground state ions are excited to a higher energy level by absorption of pump photons. These excited ions form a metastable state with an efficient transition at the signal wavelength to an intermediate energy level. From this intermediate level electrons rapidly return to the ground state by a non-radiative decay. A population inversion of the metastable state is established by pumping the fibre. When a signal photon passes the fibre stimulated emission occurs amplifying the signal.

1.2.1 Amplifiers in the 1.55 μm region

In the mid 1980s, the group led by D.N. Payne [1] at the University of Southampton developed a technology of rare earth ions deposition in single-mode silica fibres. Just when conventional unrepeatered systems had approached their peak performance they showed that optical fibres could exhibit laser gain at a wavelength near 1.55 μm. The fibres were doped with erbium (Er^{3+}) and were activated or pumped with low powers of visible light.

The nature of erbium ions is that they have some properties of radiative decay with a long excited-state lifetime in a glass host, such as the fused silica used to make optical fibres. In addition, the gain characteristics of erbium-doped fibres offer all these advantages: polarization insensitivity, temperature stability, quantum-limited noise figure, and immunity to interchannel cross talk. Later on laser diodes where used to pump the erbium-doped fibres which makes them practical as optical amplifier devices. Erbium-doped fibre amplifiers (EDFAs) where an immediate success for amplification in the 1.55 μm wavelength region.

1.2.2 Amplifiers in the 1.3 μm region

An optical amplifier working in the spectral region around 1.3 μm would be of major importance. Because the group velocity zero dispersion points falls in this region. By considering the energy levels of candidate trivalent rare earth ions three dopants; praseodymium, neodymium and dysprosium are suitable for a fibre amplifier. For all these materials, efficiency problems are encountered. None of these three rare earth ions can be used in silica. Finding a host glass material which produces an efficient amplifier is an important subject of study.

Praseodymium

For communication systems operating in the second window, a praseodymium-doped fibre is the most promising candidate. A suitable host glass material is fluoride, developed for the first time in 1990, independently by three groups: Ohishi et al. [2], Carter et al. [3] and Durteste et al. [4]. Although suited for use as amplifier, these Pr^{3+}-doped fluoride fibre versions require too much pump power. The low pump power efficiency can be attributed to the low quantum efficiency of the radiative transition of praseodymium, due to non-radiative energy transfer to lattice vibrations (phonons) of the host glass. Sulfide glasses showed obvious improvements of a praseodymium-

doped fibre amplifier (PDFA) efficiency to the fluoride glasses, given the higher radiative quantum efficiency [5].

Neodymium

Nd^{3+}-doped fluoride fibre amplifiers were early candidates as amplifiers at 1.3 μm. Unfortunately, they suffer from a host of problems and have never yielded suitable gains at wavelengths of interest for transmission applications. Despite the fact they can be pumped in the 800 nm region, where high-power laser diodes are available and the possibility of high doping concentrations that allow a short and compact device. There is a strong excited-state absorption (ESA) and a competing emission transition at 1.06 μm [6], which tends to "steal" the gain from the 1.3 μm transition. In addition, the product of the emission cross-section and the lifetime for Nd^{3+} is an order of magnitude lower than that for Er^{3+}. This indicates that the pump efficiency for an Nd^{3+}-doped fluoride fibre amplifier will be significantly lower in comparison with an Er^{3+}-doped fibre amplifier at 1.5 μm. [7]

Dysprosium

Dy^{3+}-doped materials have several large absorption bands in the near-IR region where practical pump sources are available. The stimulated emission cross-section at the 1.3 μm wavelength is in general greater than of Pr^{3+} in the same host. These factors promise relatively short fibre lengths. However, lifetime of the excited-state in Dy^{3+} is relatively short. Bottlenecking in the intermediate states and the subsequent ESA is a serious problem. Co-doping with terbium (Tb^{3+}) and alternative host materials like for instance selenide promise to overcome these problems but also introduces new problems like passive losses by increased fibre lengths [8,9,10].

1.3 Semiconductor optical amplifiers

Semiconductor optical amplifiers offer an alternative to the fibre-based counterparts, at both 1.3 μm and 1.5 μm telecommunication windows. This type of amplifier is driven by injection current. Gain is realised by electron-hole recombination induced by stimulated emission. SOAs have been realised by using InGaAsP multiple quantum wells (MQW) as active regions. By combining MQW structures under tensile and compressive strain, polarization insensitive gain has been obtained [11,12].

Despite recent considerate performance improvements, SOAs still suffer from non-linear distortions like inter-modulation distortion and cross talk. However, characteristics of SOAs that are associated with their fast non-linearities make them very attractive for a number of applications, such as optical signal processing, wavelength conversion and regeneration, time demultiplexing, clock recovery, and pattern recognition. Such all-optical functions are needed if optical networks with large-traffic-handling capacities will be developed.

1.4 Raman (fibre) amplifiers

Recent advances in grating technology and the development of high-power diode pump lasers have revived interest in Raman fibre amplifiers [13,14]. The Raman amplifier is based on the non-linear effect of stimulated Raman scattering. An undoped glass fibre core represents the gain medium. When light is transmitted to matter, it is scattered in random directions. Most of the scattered light is of the same wavelength as the incident light. This is known as "Rayleigh scattering" and is considered elastic as the scattered photon has the same energy as the incident photon.

Some light is scattered in-elastically, scattered photons having lower energy than the incident one, at a different wavelength. This is called "Raman scattering". This shifting of wavelength is called "Raman effect", which arises when incident light excites molecules in the glass fibre core, which subsequently scatters the light. In Raman amplification, an intense pump light couples to vibrational modes of the glass of fibre itself and is re-radiated at a longer wavelength, amplifying a signal if the pump is at an appropriately shorter wavelength than the signal.

Simply the pump wavelength rather than the fixed energy levels like in rare-earth fibres determine the gain spectrum. This feature allows Raman amplification to be applied across the entire transmission window of silica optical fibres. The stimulated emission coefficient is proportional to pump power density in the core. To achieve reasonable gains with currently available pump laser diodes, fibres with either small core radius or large numerical aperture (NA), not compatible with standard communication fibres, must be used.

1.5 Scope of thesis

On the project "1.3 μm Praseodymium-doped Fibre Amplifiers based on Germanium Gallium Sulfide Glasses" research is performed on an efficient optical doped-fibre amplifier based on a germanium gallium sulfide glass host doped with praseodymium.

A practical praseodymium-doped fibre amplifier (PDFA) is set-up with commercial available praseodymium-doped fluoride fibre modules. Measurements are performed to characterize the amplifier behavior, mainly focused on different amplifier configurations and amplifier applications. Different pumping schemes: co-, counter- and bi-directional propagating, as well as applications like pre-, inline and power amplification are investigated. By performing the measurements spectrally the amplifier influence on noise can be studied. The large quantity of measurements necessary would benefit from an automated testing environment.

These experimental results are used to validate an already existing praseodymium-doped fibre model that can be used to model different fibre types. A valid model can help to determine important fibre parameters and simulate amplifier behavior under different conditions. Furthermore, the model can be used to simulate the amplifier noise figure.

Furthermore, experiments are performed on a signal double-pass amplifier configuration. In this configuration a Faraday rotator mirror is placed at the end of the praseodymium-doped fibre to reflect the signal back into the active fibre. An optical circulator at the input of the amplifier directs the backward propagating signal to the amplifier output port. In this way the signal passes the doped fibre twice and benefits more from the available gain properties of the active fibre. This can result in higher signal gain compared to a single-pass set-up when the amplifier is not saturated by the signal power.

This thesis is divided in 6 chapters besides the Introduction. Chapter 2 deals with system implementations of fibre amplifiers. Different pumping schemes and amplifier applications like pre-, inline and power amplification are discussed.
In chapter 3 a praseodymium-doped fibre model is presented. The operating principles of a Pr^{3+}-doped fibre amplifier are discussed as well as amplifier efficiency decreasing processes in a Pr^{3+}-doped fibre. The theory of the model is presented, it can be used to study different fibre parameter and amplifier conditions. Next a section considering noise figure simulation using the model follows.

The next chapter is dedicated to validate the model. Experimental data collected from gain measurements on a PDFA are used in this validation. The measurements are performed on a co- and counter-directional pumped amplifier with 7 and 14 meters of Pr^{3+}-doped fluoride fibre.
Chapter 5 is dedicated to simulation results performed with the validated model and is divided into 3 sections. The first section deals with a fibre parameter sensitivity analysis. The simulation results are used to study the influence of different fibre parameters on the amplifier gain. In the second section simulation results of a bi-directional pumped amplifier are presented and the last section deals with noise figure simulation.
Experimental results, which are also used to validate the model, are discussed more into detail in chapter 6. Results on a co- and counter-directional pumped amplifier as well as a signal double-pass set-up are presented. In addition, problems are discussed encountered by determining the amplifier noise figure. Conclusions and recommendations are formulated in the last chapter of this report.

2 System implementations of fibre amplifiers

2.1 Introduction

This chapter discusses the system implementations and applications of fibre amplifiers and also some possible configurations of fibre amplifiers. The main applications have been digital, although analogue systems incorporating optical amplifiers are also of interest. The three dominant areas where the optical amplifier in general has proven invaluable are preamplification, power amplification (booster) and as inline amplifier for long-haul systems or high capacity WDM transmission links.

2.2 Preamplifiers

These amplifiers are placed in front of the receiver, to amplify telecommunications signals that are attenuated along a link and have insufficient power for error-free detection. These amplifiers operate in the so-called small signal gain regime. Signal powers around the range of –40 dBm (0.1 μW) up to –30 dBm (1 μW) are considered. Fibre amplifiers have contributed to a significant increase in the sensitivity of receivers, as compared to PIN or APD receivers alone. In the past, APD receivers where used due to their ability to provide gain. With the gain now being provided by the optical amplifier, PIN detectors become more attractive than APDs for signal to noise reasons. The quantum limited receiver sensitivity is determined by the signal-spontaneous and spontaneous-spontaneous beat noises at the output of the optical amplifier. It is an unavoidable consequence of the spontaneous emission from the amplifier. An unamplified system has a minor shot noise detection quantum limit.

The key to high sensitivity receivers is low-noise amplification. Optical preamplifiers have a clear advantage over electrical preamplifiers as they introduce significantly less noise at high gains, especially at high (greater than 1 Gb/s) bit rates. The underlying reason is that the higher the bandwidth, the harder it is to obtain low-noise operation from electronic components. For fibre-based amplifiers, low-noise amplification requires a high pump power efficiency, high signal gain per unit of absorbed pump power. A low noise figure allows for high amplification in high bit rate systems. It is also important to have a narrow bandwidth optical filter at the output of the fibre amplifier to eliminate as much amplified spontaneous emission (ASE) that exits the fibre as possible. Also by reducing the input losses, including splices, connectors, isolators and wavelength

selective couplers, the noise figure can be improved. The receiver enhancement has greatly improved with advances in the fibre amplifier performance.

More recently, preamplifiers have been demonstrated that combine very high gains with low noise figures [1,2]. These amplifiers are based on a two-stage design where two independently pumped doped fibres are separated by an isolator. In this way, the backward ASE originating from the second fibre does not travel backward and saturate the gain of the first fibre segment. As a result, much higher gains and lower noise figures are available at the signal wavelength.

2.3 Inline amplifiers

Inline amplifiers are typically used in long-haul transmission links. The signal powers are considered moderate, around –20 dBm (10 μW) up to maximum of 0 dBm (1 mW). In a transmission system, a number of issues arise that influence strongly the design of the transmission link; the type of transmission fibre used, the design of the amplifiers, and the passive components used throughout the link. Many of the performance degradation issues are related to the onset of fibre non-linearities. While fibre amplifiers offer many advantages over traditional electronic repeaters, one drawback is that they offer fertile ground for non-linearities to develop. This is due to the long interaction length that different optical pulses have in an optically amplified link as well as the higher optical powers. While it is desirable to have high signal power to ensure a good signal-to-noise ratio (SNR) at the receiver, once the power too high, non-linearities begin to accumulate, degrading system performance.

2.4 Booster amplifier

These amplifiers are located at an optical transmitter and can boost a transmitter signal to the required power level. The operating regime of power amplifiers is called the large signal gain regime or saturation regime. Normally signal powers of 0 dBm (1 mW) or higher are considered as being large. So booster amplifiers are typically used to amplify signal with more power than is the case for preamplifiers. A high pump to signal power conversion efficiency and a high saturation level are the prime requirements. Improvements have been obtained in power amplifier performance by means of fibre amplifiers. These booster amplifiers are also used in multi-way power splitting and amplification to achieve loss-less splitting like in analogue systems for television signal broadcasting. These analogue systems require very high signal to noise ratios so

the signal levels are kept high. But, in order to keep the noise figure low care must be taken not to saturate the amplifier by means of too high signal powers.

2.5 Non-linear effects

Although no non-linearities are examined for the PDFA, still some non-linear effects hampering amplifier behaviour are described [3].

Four-wave mixing:

The first major problem that can arise in an amplified link is four-wave mixing between the optical pulse and the ASE of the amplifiers. When the two fields propagate together, as in the case when the signal wavelength is around the zero dispersion point of the transmission fibre, then significant spectral broadening and distortion of the pulse occurs. Effectively, most of the signal pulse energy gets absorbed in optical filters used in the system (the fibre amplifier bandwidth also acts like a filter), as the edges of the broadened signal spectrum get clipped. For transmission system using a WDM scheme also four-wave mixing between the different channels occurs.

Self-phase modulation:

In general, the refractive index of a medium is intensity dependent. Under most conditions this can be neglected except when pulse intensity becomes too large. This causes self-phase modulation (SPM) and results in pulse broadening. Coupled with group velocity distortion this will create temporal pulse distortion if a large amount of dispersion is accumulated over the entire system length. In the context of WDM systems an effect, based on the same physical principles as self-phase modulation called cross-phase modulation occurs. Intensity variations in one pulse alter the phase of another channel, via the non-linear refractive index of glass. This also leads to spectral broadening.

Stimulated Brillouin scattering:

This arises from the interaction between a photon and an acoustic phonon. The backscattering event involves the scattering of a photon of lower frequency with the simultaneous creation of a phonon. The light created by this process propagates in a direction counter to that of the signal and is amplified with distance as the photons stimulate the creation of more photons of the same frequency. This process robs signal photons and thus increases the noise due to the fact that the signal power decreases and the random removal of photons is equivalent to the addition of random noise.

Polarisation effects:

However fibre amplifiers do exhibit a very weak polarization-dependent gain, in the case of long-haul systems, this becomes significant when many amplifiers are cascaded. There are three main polarization effects: polarization-dependent loss, polarization-dependent gain and polarization mode dispersion effects.

Stimulated Raman scattering:

Also stimulated Raman scattering can become a problem. This scattering is similar to stimulated Brillouin scattering but differs in that the scattering event is between a photon and an optical phonon [4]. Optical phonons have much higher frequencies and energies than acoustic phonons. The light induced by the Raman scattering can propagate in the forward direction and is amplified by the signal as they propagate together. In a WDM system, stimulated Raman scattering will impair the system performance by providing a way by which energy can be transferred between the different WDM channels [5].

2.6 Amplifier configurations

These different amplifier applications can be achieved by some basic amplifier configurations. The most common are the co-propagating, the counter-propagating and the bi-directional pumping scheme as shown in figure 2.6.1.

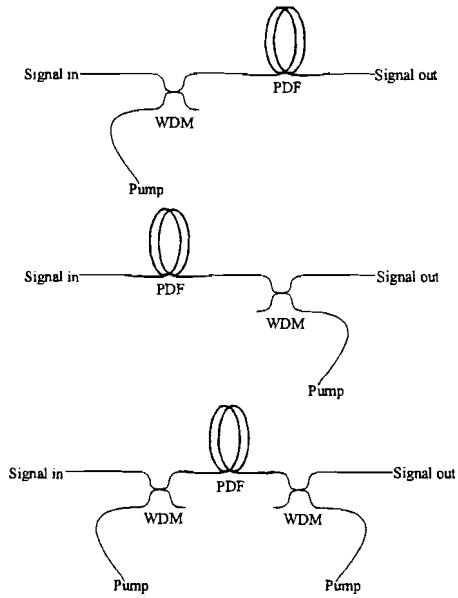

Figure 2.6.1: Some possible amplifier pump configurations. Top: co-propagating, middle: counter-propagating and bottom: bi-directional pump scheme.

The direction depends depicts how pump and signal propagate along the praseodymium-doped fibre (PDF), a WDM is used to couple the pump power. The configurations above all have their advantages and disadvantages mainly determined by the application for which they are used. Influence of the active fibre parameters like for instance background loss, doping concentration and length are examined in chapter 5. Also the influence of pumping scheme on the signal gain and the amplifier noise behaviour are of great importance. These factors will be handled more into detail in chapter 6.

In [6,7,8] a double-pass configuration is suggested. Here the signal is reflected back at the output side of a bi-directional pumped amplifier using a mirror or grating. This mirror can be a Faraday rotator mirror (FRM). At the input side the double-passed signal is split from the incoming signal by an optical circulator. The signal will pass the doped fibre twice, making more efficient use of the available fibre gain. This only applies for the small signal gain regime. If the amplifier saturates, the output power will be limited by the available pump power.

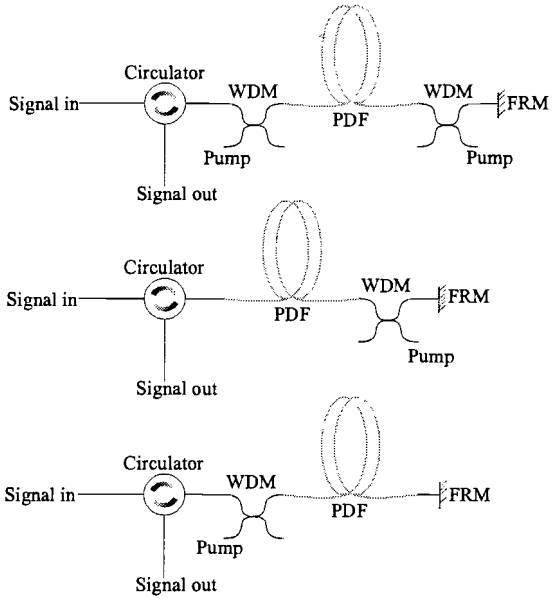

Figure 2.6.2 Possible double-pass configurations. Top: bi-directional, middle: counter-propagating and bottom: co-propagating pumped scheme.

In figure 2.6.2 some possible double-pass set-ups are shown. Instead of only reflecting the signal power it is also possible to re-use the pump power or both signal and pump power. The most suitable configurations highly depend on the total pump power available, the length of the doped fibre and the desired application. Experimental results are presented in chapter 6.6.

3 Modelling of the praseodymium-doped fibre amplifier

3.1 Introduction

A steady state praseodymium-doped fibre amplifier model is presented in this chapter. First the basic principles of operation of a praseodymium-doped fibre are discussed. Also amplifier efficiency decreasing processes are discussed. From this a model is derived, based on a simplified energy level diagram. The relevant powers in the doped-fibre are spectral as well as spatially resolved. These powers are the signal power, forward and backward travelling pump powers and amplified stimulated emission (ASE) that also travels in both directions. The model can be used in many different operating conditions like co-directional, counter-directional or bi-directional pumping. The amplifier model can also be used for noise figure simulations.

3.2 Operating principles

The optical fibre amplifier operates by the same fundamentals as a laser, which is light amplification by stimulated emission of radiation. It is based on materials that can produce optical gain. There are some necessary requirements to achieve optical gain. A metastable state must exist in the material having a radiative transition that matches the wavelength of the light that is to be amplified. This has to be an efficient and relatively large transition in comparison with the non-radiative rate. And at last, there must be a way to populate the upper of the two levels by pumping the amplifier with a light-source of a shorter wavelength.

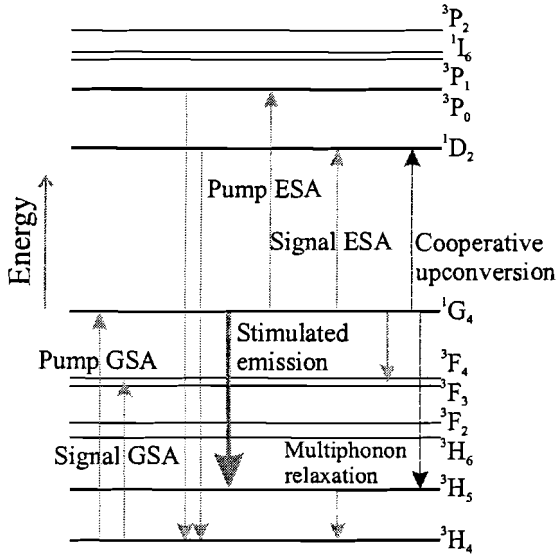

Figure 3.2.1 The energy level diagram of Pr^{3+} in a glass host. Essential transitions are indicated.

For discussing the operation of the PDFA, a closer look is taken at the energy level diagram of praseodymium in a glass host as depicted in figure 3.2.1. Not indicated in the figure, but due to Stark splitting and homogeneous broadening the energy levels are no longer sharp lines, but they are split into many sublevels and form energy bands. Amplification is achieved by establishing a population inversion between the $^1G_4$ and $^3H_5$ levels of ionised praseodymium. This inversion can be achieved, with differing efficiencies, by pumping the Pr^{3+}-ion from the ground state $^3H_4$ to the excited $^1G_4$ state, at wavelengths anywhere between 950 and 1050 nm. In optical amplified systems like rare earth-doped glasses, the pump-excited-state decays into a metastable state, as the system returns to the ground state. In the Pr system the $^1G_4$ state happens to be both the pump-excited-state and the metastable state.

The PDFA exhibits a long emission lifetime of the metastable state. This permits a large population inversion, in which almost all ions are excited in the metastable state instead of in the ground state, needed to achieve high gain. The radiative transition from the $^1G_4$ to the $^3H_5$ state is active around 1.3 μm [1]. The transition can be induced by a signal, containing photons with the same energy, to produce stimulated emission. The process of stimulated emission provides amplification of the signal. The figure below illustrates the stimulated emission process.

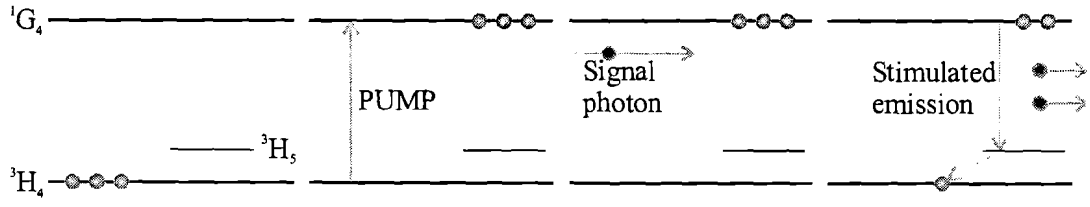

Figure 3.2.2 The process of stimulated emission in Pr^{3+}-doped glass. Praseodymium ions in the ground state $^3H_4$ are excited to the metastable $^1G_4$ state by absorption of pump photons. When a signal photon travels through the doped fibre, stimulated emission at the signal wavelength occurs. The excited Pr ion quickly returns to the ground state by non-radiative multiphonon relaxation from the $^3H_5$ state.

From the $^3H_5$ state the excited Pr^{3+} ions quickly return to the ground state. Due to this fast depopulation, the $^1G_4$ state may easily become highly populated relative to the $^3H_5$ state and population inversion is readily achieved. If stimulated emission does not occur, then the transition eventually will take place spontaneously, radiating photons of random phase and direction. A fraction of the spontaneous emitted photons is captured by the fibre mode and travels in both directions along the fibre. These photons are subsequently amplified in the same way as the signal and results in ASE. The ASE power integrated across the PDFA gain spectrum can be quite

substantial resulting in the main part of the amplifier noise. Although three levels are involved, the amplifier is called a four level-operation, because the $^1G_4$ state doubles as the pump-excited and the metastable state.

3.3 Amplifier efficiency decreasing processes

Apart from these fundamental transitions, which are responsible for amplification, other transitions take place. Any process other than stimulated emission, removing Pr^{3+} ions from the $^1G_4$ level and depopulating this upper amplifier level, necessarily decreases the efficiency of an amplifier. Thus the degree to which population inversion is established determines the amplifier efficiency.

Possible gain-limiting processes could be excited-state absorption (ESA) transitions by absorption of either pump or signal photon. Signal ESA is the excitation of an ion in the $^1G_4$ state to the $^1D_4$ state through the absorption of a signal photon. This could result in a reduction of pump efficiency. From the $^1D_2$ level, an amount of electrons will subsequently fall non-radiatively to the $^3F_4$ or $^3F_3$ levels. Pump ESA excites a Pr^{3+} ion in the $^1G_4$ state to the $^3P_0$ state. As a consequence one pump photon and one excited-state are lost. From levels $^1D_2$ and $^3P_0$ (or $^3P_1$, $^3P_2$) the radiative emission in the ground state $^3H_4$ is most probable [2]. These transitions emit light in the visible range and so the pumped fibre shines red.

Another loss mechanism is the signal ground-state absorption (GSA) transition by absorption of a signal photon to the $^3F_4$ or $^3F_3$ state. This signal photon does not contribute in a useful way, as Pr decays from the $^3F_4$ level by cascaded non-radiative multiphonon relaxation decay. This can only occur if there are any electrons in the ground state. If the population inversion is inverted ground-state absorption will be bleached.

Another transition is the non-radiative transition from the $^1G_4$ to the $^3H_4$ ground state, either directly or via one or more of the $^3F_4$, $^3F_3$, $^3F_2$, $^3H_6$ or $^3H_5$ levels, by multiphonon relaxation, i.e. by excitation of several lattice vibrations or phonons. The lifetime of the $^1G_4$ level is called the spontaneous emission lifetime τ, the time in which the population falls to 1/e of its original value. Multiphonon relaxation decreases the spontaneous emission lifetime of the metastable state and is therefore an unwanted phenomenon.

In Pr^{3+}-doped glass, several ion-ion interactions exist that can quench the Pr luminescence and decrease the emission lifetime, and can thus reduce the amplifier efficiency. Concentration

quenching occurs through the mechanism of cross relaxation [3]. In this process an excited Pr^{3+} ion transfers part of its energy to excite a second ion from the ground state, leaving both in an intermediate state. Both ions will subsequently decay non-radiatively to the ground state by multiphonon relaxation. This process is independent of pump power because of the involved ground state ion.

In principle, a doping concentration as high as possible is desired. This would lead to very short fibre lengths, which is an advantage of practical use and costs. Furthermore the amplifier would be less hampered by the fibre background loss. But this idea is too straightforward. If the concentration becomes too high, the average distance between two adjacent excited praseodymium ions becomes too small. Interacting by co-operative upconversion [4,5] can take place. In this process, energy transfer takes place between two neighbouring ions in the metastable state, promoting the acceptor to the $^1D_2$ state and demoting the donor to the $^3H_5$ state by non-radiative energy transfer. As a result two excited-states are lost. Therefore, the spontaneous emission lifetime of the $^1G_4$ level will decrease. Thus the upconversion rate depends on the concentration of excited Pr^{3+}-ions. Upconversion will therefore be evident at high pump powers and Pr^{3+} concentrations.

Just like in ordinary transmission fibres, light will also be lost by scattering against impurities within the glass and by absorption of various chemical bonds, e.g. the O-H bond that also quenches Pr^{3+} concentration. These losses are generally much higher in doped fibres. It is difficult to obtain the high-purity starting materials as well for the glass composition as for the doping. Good Pr^{3+}-doped fibres still have background loss of 0.1 – 0.5 dB/m, hundred of times more than transmission fibres. Fortunately, only limited lengths are needed for a practical amplifier.

3.4 Fibre amplifier modelling

3.4.1 Introduction

This section describes a fibre amplifier model as mentioned in [6], the used model is based on the article by Karasek [7]. Equations will be presented for a model, which can be used to study the amplifier operation in different configurations and under different conditions. Simulation conditions like pump power, signal power or signal wavelength are used to calculate output signal and ASE powers. The model can also be used to optimise the design of praseodymium-doped fibres. Possible simulation variables are fibre length, cut-off wavelength and numerical aperture. Specifications of fibre parameters are used to characterise the active fibre, appendix A is an example of fibre specification supplied by the manufacturer. The level transitions can be completely characterised by

their cross-section spectra and spontaneous emission lifetimes. Data from photo-luminescence measurements on the active fibre are converted as input files for the model. The cross-sections used are signal emission, signal ground state absorption, signal excited-state absorption, pump absorption and also background losses are taken into account.

3.4.2 PDFA model

ASE contributions at all wavelengths must be taken into account, because of the possibility of saturation of the amplifier by the ASE noise. The ASE spectrum is made discrete into a number of sections. For each section, the optical power versus distance within the fibre has to be calculated. Figure 3.4.1 shows a typical amplifier output spectrum with ASE contribution and the division into wavelength sections.

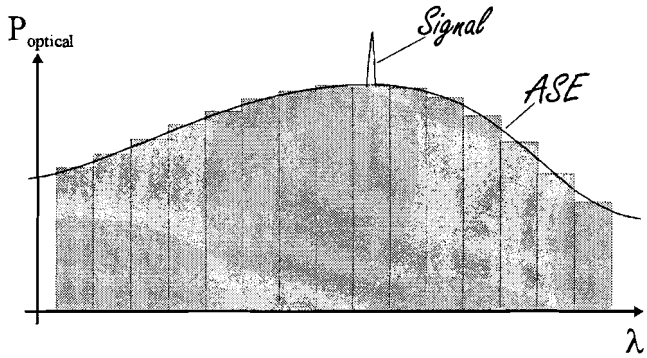

Figure 3.4.1 Typical amplifier output spectrum. The model divides the amplified spontaneous emission spectrum into a number of wavelength sections.

The fibre geometry, relevant to optical propagation, can be described completely using two parameters. These are the fibre's numerical aperture (NA) and cut-off wavelength (λ_c). The core radius (a) is related to the NA and λ_c by:

$$a = \frac{2.405\lambda_c}{2\pi NA} \quad [\text{m}] \tag{3.1}$$

In addition, an important fibre parameter is the doping distribution. In the simplest fibres the doping distribution is uniform across the fibre core cross-section. To find the optimum fibre structure, the mode profiles of pump and signal must be evaluated. The core area of the fibre is divided in a number of concentric rings as depicted in figure 3.4.2. For each ring the optical intensities of pump, signal and ASE-sections are calculated using the total powers and the mode profiles.

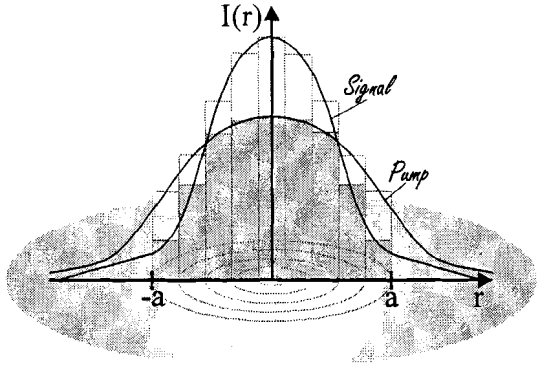

Figure 3.4.2 Fibre surface segment with core radius a. Pump and signal mode profiles are outlined. The overlap of both profiles is filled in. The division into rings of the fibre core and the quantisation of the light intensity is shown.

The level transitions can be completely characterised by their cross-section spectra and spontaneous emission lifetimes. The spontaneous decay from a certain level I, is given by the constant τ_I. All radiative and non-radiative decay channels starting from level I determine this constant. The cross-section is a measure of the strength of an induced transition (absorption or emission) at a certain wavelength. The transition rate W_{IK} between level I and K can be expressed as [8]:

$$W_{IK}(x,y,z) = \int_0^\infty \sigma_{IK}(\nu)\frac{I(\nu,x,y)}{h\nu}P(\nu,z)d\nu \qquad [s^{-1}] \tag{3.2}$$

Where σ_{IK} is the section involved. P(ν,z) is the optical power spectral density [W/Hz] over the fibre's cross-section. I(ν,x,y) is the transverse intensity distribution of the optical mode at frequency ν, normalised to:

$$\iint I(\nu,x,y)dxdy = 1 \tag{3.3}$$

The normalised intensity in the fibre core is calculated as [9]:

$$I(\nu,r) = \frac{1}{\pi}\left[\frac{\upsilon}{aV}\frac{J_0\left(\frac{ur}{a}\right)}{J_1(u)}\right]^2 \qquad [m^{-2}] \tag{3.4}$$

Where J_0 and J_1 are the zero order and first order Bessel functions of the first kind, u is the transverse propagation constant and υ the transverse decay constant. The V-number or normalised frequency at wavelength λ (= c/ν) is:

$$V = \frac{2\pi a}{\lambda} NA \qquad [\mathrm{m}^{-1}] \tag{3.5}$$

The value of υ cannot be calculated analytically, it is found by interpolation from a table given in [7]. A linear approximation is often used to find υ, but this is not accurate for small values of V. The transverse propagation constant u is related to V and the transverse propagation constant υ by:

$$u = \sqrt{(V^2 - \upsilon^2)} \qquad [\mathrm{m}^{-1}] \tag{3.6}$$

Figure 3.4.3 shows the relevant transitions that are used by the model.

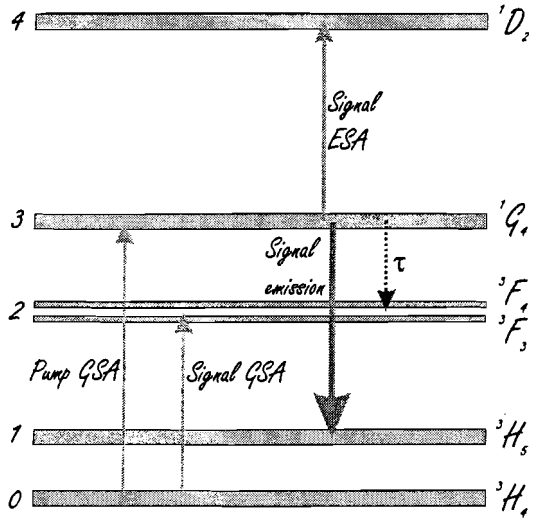

Figure 3.4.3 Essential transitions used by the model. Pump ground state absorption, signal excites state absorption and signal emission, as well as the spontaneous emission lifetime τ.

The rate equations describe the transition rates between the various levels in the doped material.

The pump absorption rate is:

$$W_{03}(r,z) = \sigma_{03}(\nu_p)\frac{P_p^+(z) + P_p^-(z)}{h\nu_p} I(r,\nu_p) \qquad [s^{-1}] \tag{3.7}$$

Where $\sigma_{03}(\nu_p)$ is the pump absorption cross-section at the pump frequency ν_p. Integration over ν is not required as the pump is assumed to have one single wavelength. $P_p^+(z)$ is the pump power propagating in the forward and $P_p^-(z)$ is the pump power propagating in the backward direction. The stimulated emission rate due to signal and ASE, using the stimulated emission cross-section $\sigma_{31}(\nu)$, is given by:

$$W_{31}(r,z) = \int_{c/\lambda_{min}}^{c/\lambda_{max}} \sigma_{31}(\nu)\frac{P_{ase}^+(z,\nu) + P_{ase}^-(z,\nu)}{h\nu} I(r,\nu)d\nu + \sigma_{31}(\nu_s)\frac{P_s(z)}{h\nu} I(r,\nu_s) \qquad [s^{-1}] \tag{3.8}$$

A single wavelength signal ν_s is assumed. $P_{ase}^+(z,\nu)$ and $P_{ase}^-(z,\nu)$ are the forward and backward propagating noise power spectral densities. $P_s(z)$ is the signal power. The noise (ASE) is integrated over the wavelength range $\lambda_{min} - \lambda_{max}$. Finally, the excited-state absorption rate follows from a similar equation:

$$W_{34}(r,z) = \int_{c/\lambda_{min}}^{c/\lambda_{max}} \sigma_{34}(\nu)\frac{P_{ase}^+(z,\nu) + P_{ase}^-(z,\nu)}{h\nu} I(r,\nu)d\nu + \sigma_{34}(\nu_s)\frac{P_s(z)}{h\nu} I(r,\nu_s) \qquad [s^{-1}] \tag{3.9}$$

$\sigma_{34}(\nu)$ is the excited-state absorption cross-section. The transition rate for signal ground state absorption does not need to be evaluated as the ions rapidly fall back into ground state. Only transitions that effect the population inversion are needed.

In the steady state situation, equilibrium will be reached between the various transition rates. This means the population densities will no longer change. The amplification of the active fibre depends of the population inversion between the $^1G_4$ and $^3H_4$ state. Given this, expressions can be derived for the population densities of the metastable level and ground state levels:

$$\eta_3(r,z) = \rho(r)\frac{W_{03}(r,z)}{W_{03}(r,z) + W_{34}(r,z) + W_{31}(r,z) + 1/\tau} \qquad [m^{-3}] \tag{3.10}$$

$$\eta_0(r,z) = \rho(r) - \eta_3(r,z) \qquad [\mathrm{m}^{-3}] \tag{3.11}$$

$\eta_3(r,z)$ and $\eta_0(r,z)$ are the densities of Pr^{3+}-ions in the $^1G_4$ and $^3H_4$ states respectively. The total density of Pr^{3+}-ions is $\rho(r)$ and τ is the spontaneous emission lifetime. When the population densities and population inversion are known, the propagation of pump, signal and ASE can be determined. In [7] propagation equations are given for PDFAs. The propagation equations are used to describe the evolution of optical powers versus travelled distance. This model also includes a signal ground state absorption factor $g_g(z,\nu)$ that is a population inversion dependent factor and a factor $\alpha(\nu)$ for background loss that is independent of the population inversion. The propagation equations becomes:

$$\frac{dP_p^{\pm}(z)}{dz} = \mp[g_p(z) + \alpha(\nu_p)]P_p^{\pm}(z) \qquad [\mathrm{Wm}^{-1}] \tag{3.12}$$

$$\frac{dP_s(z)}{dz} = [g_e(z,\nu_s) - g_a(z,\nu_s) - g_g(z,\nu_s) - \alpha(\nu_s)]P_s(z) \qquad [\mathrm{Wm}^{-1}] \tag{3.13}$$

$$\frac{dP_{ase}^{\pm}(z,\nu)}{dz} = \pm[g_e(z,\nu_s) - g_a(z,\nu_s) - g_g(z,\nu_s) - \alpha(\nu_s)]P_{ase}^{\pm}(z,\nu) \pm 2h\nu\Delta\nu g_e(z,\nu)$$
$$[\mathrm{Wsm}^{-1}] \tag{3.14}$$

Where $\Delta\nu$ is the bandwidth of the wavelength section being considered. Equations (3.12) to (3.14) must be integrated to find the pump, signal and ASE powers versus distance within the fibre. Equation (3.12) consists actually of two equations; one for co-propagating and one for counter-propagating pump power. Equation (3.14) has to be solved for each wavelength section of the ASE spectrum and for both directions of propagation. The pump ground state absorption, signal/ASE stimulated emission, signal/ASE excited-state absorption and signal/ASE ground state absorption factors are given by:

$$g_p(z) = 2\pi\sigma_{03}(\nu_p)\int_0^a \eta_0(r,z)I(r,\nu_p)rdr \qquad [\mathrm{m}^{-1}] \tag{3.15}$$

$$g_e(z,\nu) = 2\pi\sigma_{31}(\nu)\int_0^a \eta_3(r,z)I(r,\nu)rdr \qquad [m^{-1}] \tag{3.16}$$

$$g_a(z,\nu) = 2\pi\sigma_{34}(\nu)\int_0^a \eta_3(r,z)I(r,\nu)rdr \qquad [m^{-1}] \tag{3.17}$$

$$g_g(z,\nu) = 2\pi\sigma_{02}(\nu)\int_0^a \eta_0(r,z)I(r,\nu)rdr \qquad [m^{-1}] \tag{3.18}$$

The preceding equations must be solved with numerical methods to find an approximate solution. For each integration step of the propagation equations, the different absorption factors have to be evaluated first. And for this the population densities at the different levels are required. To do this the different transition rates are calculated. These last equations use all signal, pump and ASE powers, so completing the circle.

3.4.3 Noise figure theory

This section is based on the publication of Olsen [11] and the report written by Nabuurs [12] who adapted the fibre amplifier model for noise figure simulations. An important parameter to describe the performance of a system is the noise figure F, which is defined as:

$$F = 10^{10} LOG\left(\frac{SNR_{in}}{SNR_{out}}\right) \qquad [dB] \tag{3.19}$$

Where SNR_{in} is the signal to noise ratio at the input of the system and SNR_{out} is the signal to noise ratio at the output of the praseodymium-doped fibre amplifier.

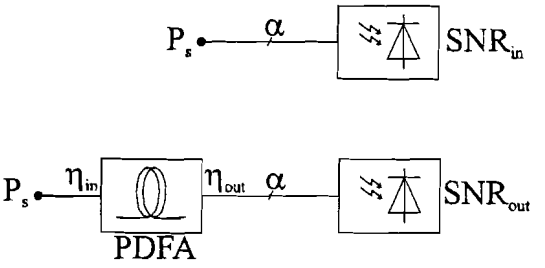

Figure 3.4.4 Schematic of signal-to-noise ratios used in noise figure simulation

If a photodiode as detector is considered then the SNR_{in} is defined as the SNR at the output of the photodiode, when the input signal (P_s) is directly fed to this detector. The signal power after the detector is proportional to the square of the signal current (I_s). If a detector photodiode with no thermal noise is assumed, then the main noise of the detector photodiode is the shot-noise (N_{shot}). The equations for signal current and shot-noise are:

$$I_s = \frac{P_s e \eta \alpha}{h\nu} \quad [\mathrm{A}] \tag{3.20}$$

$$N_{shot} = 2eI_s B_e \quad [\mathrm{A}^2] \tag{3.21}$$

Where e is the elementary charge, η is the photodiode quantum efficiency, α is the optical loss of the fibre connected to the input of the detector, h is Planck's constant, ν the frequency of the optical signal and B_e the electrical bandwidth. From equation (3.20) and (3.21) we find:

$$SNR_{in} = \frac{I_s^2}{N_{shot}} = \frac{P_s \alpha \eta}{2h\nu B_e} \tag{3.22}$$

The SNR_{out} is defined as the SNR at the output of the detector, when the detector is connected to the output of the PDFA that is fed with the input signal (P_s). In this case, the signal current at the output of the detector is:

$$I_s' = \frac{G P_s \eta_{in} \eta_{out} \alpha e \eta}{h\nu} \quad [\mathrm{A}] \tag{3.23}$$

Where G is the gain of the PDFA, η_{in} is the input coupling loss and η_{out} the output coupling loss. After detection the received signal power is given by the square of I'_s. The current caused by the forward ASE power (P_{sp}) is:

$$I_{sp} = \frac{P_{sp} \alpha \eta_{out} e \eta}{h\nu} \quad [\mathrm{A}] \tag{3.24}$$

For a detector diode that produces no thermal noise, the total noise at the detector output consists of shot-noise, signal spontaneous noise ($N_{s\text{-}sp}$) and spontaneous-spontaneous noise ($N_{sp\text{-}sp}$). The equations are:

$$N_{shot} = 2e(I_s^{'} + I_{sp})B_e \qquad [A^2] \tag{3.25}$$

$$N_{s-sp} = \frac{4I_s^{'}I_{sp}B_e}{B_o} \qquad [A^2] \tag{3.26}$$

$$N_{sp-sp} = \frac{2I_{sp}^2(B_0B_e - \frac{1}{2}B_e^2)}{B_0^2} \qquad [A^2] \tag{3.27}$$

From equation (3.23) to (3.27) is found:

$$SNR_{out} = \frac{\left(\frac{GP_s\eta_{in}\eta_{out}\alpha e\eta}{h\nu}\right)^2}{\frac{2e(GP_s\eta_{in}+P_{sp})e\eta\alpha\eta_{out}B_e}{h\nu} + \frac{4(\alpha\eta_{out}\eta e)^2GP_s\eta_{in}P_{sp}B_e}{(h\nu)^2B_0} + \frac{2(\alpha\eta_{out}\eta eP_{sp})^2(B_0B_e - \frac{1}{2}B_e^2)}{(h\nu)^2B_0^2}} \tag{3.28}$$

Substituting the equations (3.19), (3.22) and (3.28) gives the equation for calculating the noise figure of the PDFA:

$$F = 10LOG\left(\frac{\alpha\eta}{\eta_{in}^2}\left[\frac{GP_s\eta_{in}+P_{sp}}{G^2P_s\eta_{out}\alpha\eta} + \frac{2P_{sp}\eta_{in}}{GhvB_0} + \frac{(B_0 - \frac{1}{2}B_e)P_{sp}^2}{G^2P_shvB_0^2}\right]\right) \qquad [dB] \tag{3.29}$$

If the PDFA is used in combination with a filter at its output, then P_{sp} equals the ASE power at the PDF-output within the optical bandwidth of the filter. The coupling loss of the filter may be accounted for by adapting the value of η_{out}.

3.4.4 Noise figure simulation

After solving the PDFA boundary problem, all ASE powers of each wavelength band are known as well as the gain. The ASE spectrum of concern is in the range from 1250 nm to 1350 nm and is divided into wavelength bands. The ASE spectrum is generally smooth, so the ASE power within each band is assumed to be equally divided. As input for a noise figure simulation the values for α, η_{in}, η_{out}, η and B_e are needed. The signal frequency ν is calculated as follows:

$$\nu = \frac{c}{\lambda_s} \qquad [s^{-1}] \tag{3.30}$$

Where c is the speed of light. The signal wavelength λ_s is constant and the signal power P_s is the variable for the simulation. The methods used for calculation of B_0 and P_{sp} depend on whether an optical filter is used at the output of the PDFA. If a filter is used, the centre wavelength of the optical filter is assumed to be equal to the signal wavelength. P_{sp} equals the ASE power at the PDFA output within the bandwidth of the optical filter. The ASE power contributed by a band partially within the range of the optical bandwidth is calculated as follows. The overlap in wavelength between the filter band and ASE slot is divided over the range of wavelength band and multiplied by the band ASE power. If no filter is used, the maximum ASE power is searched for and then an approximate -3 dB bandwidth is determined and used as value for B_0. P_{sp} is found by summarising the ASE powers in this band.

4 Experimental validation of model

4.1 Introduction

In this chapter the results obtained from simulations using the doped-fibre model are validated with measured data. This is done for both co-propagating and counter-propagating pump schemes configurations with a total of 7 m or 14 m of active fibre length. Results over a wide spectral signal range are discussed. The model only describes an active doped-fibre, so to validate it, all experimental data must be compensated for power losses back to the fibre input and output connections. From this point on the active fibre refers to simulated results where the praseodymium-doped fibre (PDF) module refers to experimental results. In the figure below cross-section data of the PDF module used in the simulations are shown.

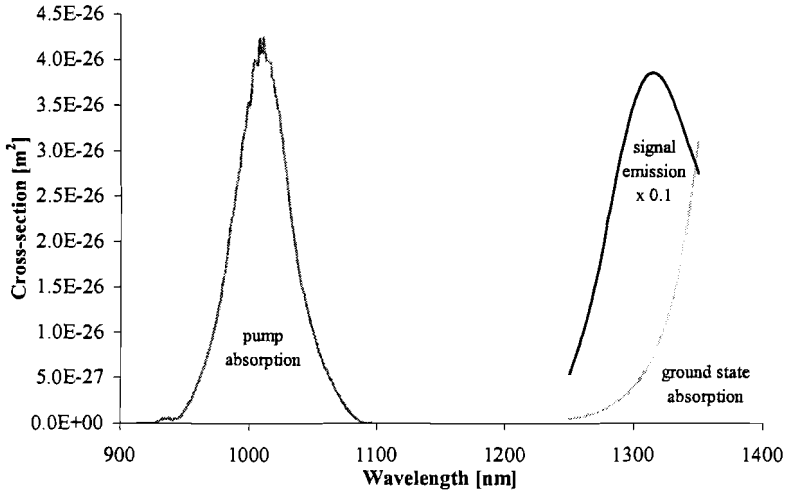

Figure 4.1 Cross-section data used by model to describe the active fibre. Displayed are the pump absorption, the ground state absorption (GSA) and the signal emission cross-section. The last one is scaled with a factor 0.1.

These cross-sections are extracted from photo-luminescence measurements and converted into input files for the model. The excited-state absorption (ESA) cross-section is missing in this figure. At this time the ESA data for the used fibre is not available. The model needs an ESA data file as input for simulations so a very small constant value of 10^{-30} m^2 is chosen for the simulations, subsequently neglecting the influence of ESA but preventing numerical errors caused by missing ESA data. The pump absorption cross-section peaks around 1011 nm, so this would be the most efficient wavelength for the pump source. The signal emission cross-section shows a peak just above 1300 nm. Remotely from the point where ground state absorption has to be taken into

account, the highest signal gain is expected around this wavelength. Other parameters that describe the active fibre, extracted from appendix A are listed in table 4.1.

Table 4.1 Fibre parameters used to describe the active fibre.

Parameter	*Value*
Numerical aperture NA	0.182
Cut-off wavelength λ_c	950 nm
Peak doping concentration ρ_{peak}	2.4 10^{25} ions/m^3
Background loss α	0.1 dB/m
Emission lifetime τ	130 μs

4.2 Gain measurements

For the different gain measurements the set-up of figure 4.2 is used. The signal input/output ports are defined when the pump direction is chosen. This also applies for the isolator orientation as depicted in figure 4.2.1. Situation 1 is for a co-propagating pump scheme and situation 2 is a counter-propagating pump scheme.

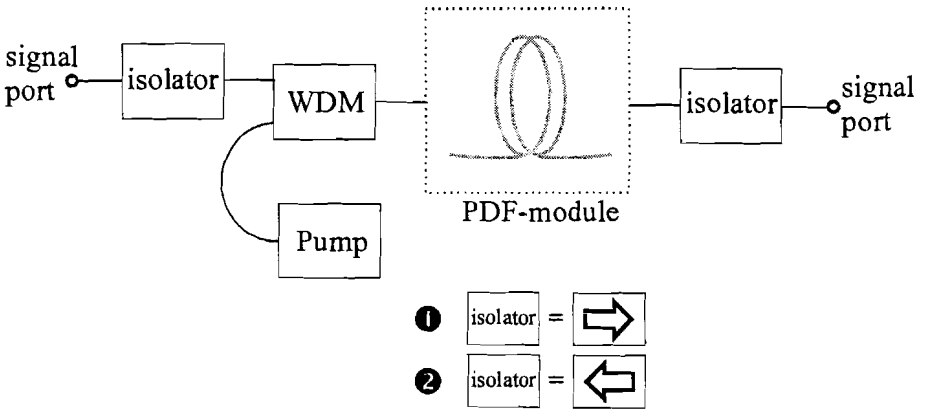

Figure 4.2 Experimental set-ups to perform gain measurements. Situation 1 is a co-propagating pump scheme and situation 2 a counter-propagating pump scheme. The signal ports changes from input to output port.

An ytterbium fibre laser (YFL) operating at 1030 nm is used as pump source. The signal is generated by a combination of tunable laser source and an optical attenuator. The signal and pump powers are combined in a 1030/1300 nm WDM. When in the next paragraphs following a pump power value is mentioned, the actual power coupled into the fibre module is meant. Each PDF module contains 7 m of In-based fluoride fibre. At the fibre ends silica pigtail fibre is spliced to make the outside connection. The set-up can consist out of one PDF module or a cascade of two

modules resulting in a total doped-fibre length of 14 m. The powers are measured with an optical spectrum analyser (OSA). The signal gain is determined by the difference between input power and output power. A major advantage of gain measurements with an OSA instead of a power meter is the possibility to leave out optical band pass filters. These filters are necessary to filter out ASE contribution when using a power meter. These measurement instruments and signal and pump source are controlled by a computer to automate the gain measurements. This measurement set-up is discussed in detail in appendix B.

The measurements on an amplifier configuration are performed as complete sets before a different amplifier configuration is being measured. This is done to prevent coupling inaccuracies introduced by changing pump scheme or fibre length. Expected inaccuracy for the output power is ±0.2 dB caused by the OSA. For the input power this is ±0.5 dB caused by a combination of uncertainties from laser source and optical attenuator and the OSA inaccuracy. For the total pump power coupled into the PDF module an inaccuracy of ±0.4 dB is expected, caused by inaccuracies of the pump power tap point ratio and power meter, also the stability of pump source power over time introduces inaccuracies.

To validate the PDFA model all experimental data must be compensated for power losses introduced by isolators, WDM, patch cords and connections, to determine the powers at the active fibre ends. This also introduces inaccuracies and uncertainties caused by wavelength dependence behaviour of some components. When co-directional pumped an input signal inaccuracy of ±0.7 dB is expected and for the output signal ±0.4 dB. The difference in accuracy is caused by the WDM, when counter-directional pumped these values are exchanged from input to output port. No compensation in pump power is necessary, in the measurement set-up the pump power is already defined at the input of the PDF module.

4.3 Co-propagating pump scheme

The total fibre loss is plotted in figure 4.3.1 versus signal wavelength for different fibre lengths. The main losses are caused by the fibre background losses and coupling losses. Also the ground state absorption of the doped fibre reduces signal power, mainly at the higher wavelengths.

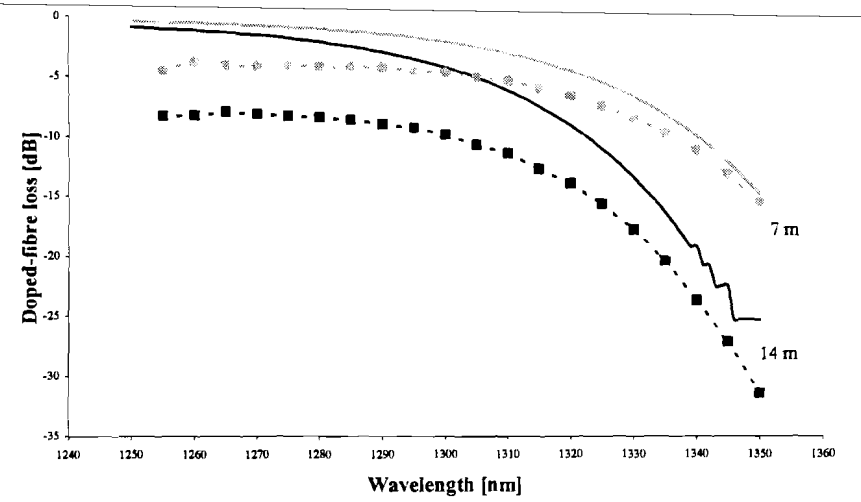

Figure 4.3.1 Doped-fibre loss when no pump power is applied with 7 m (grey) and 14 m (black) of fibre and a signal power of −30 dBm. Solid lines represent simulated and dashed lines experimental results.

For 7 m of active fibre a large mismatch between measurement and simulation data is present especially in the lower wavelength region. At 1300 nm the mismatch is 2.6 dB but decreases at higher wavelengths. The difference for 14 m of active fibre has become even worse, at 1300 nm the mismatch is 5.6 dB but also decreases at higher wavelengths. All simulation results presented in this chapter are unwittingly performed with a background loss of 0.03 dB/m. This value is too small, from appendix A it follows that the combination of scattering loss and background loss results in a total loss of 0.2 dB/m. Splicing losses (2 x 0.5 dB) and coupling losses caused by mode mismatches are also neglected.

The observed mismatch can be explained partly by a combination of simulating without taking any coupling and splicing losses into account and a too small value chosen for the background loss of the fibre. The total sum of these losses is referred to as the fibre intrinsic loss. In the next chapter an extensive analysis is performed concerning the influence of some important doped-fibre parameters like the fibre background loss.

Figure 4.3.2 depicts the small signal gain spectrum for different pump power values. The left side is for 7 m and the right side is for 14 m of fibre. In general, there is a good match between the shapes of the gain profiles and also amongst the relative placement of the profiles.

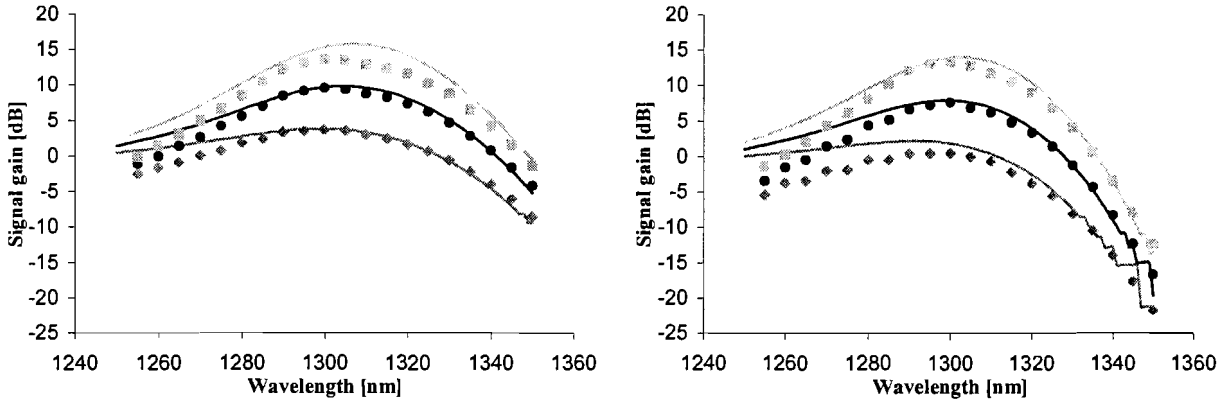

Figure 4.3.2 Small signal gain spectrum for co-propagating pump with 100 mW (◆), 200 mW (●) and 300 mW (■) of pump power. Signal power is –40 dBm. Left side is 7 m and right side 14 m of fibre. Solid lines represent simulated and markers experimental values.

A mismatch in small signal gain is present especially for low wavelengths. For 7 m of fibre length the maximum mismatch at 1270 nm is 2.2 dB for 300 mW of pump power. In the wavelength range between 1300 nm and 1330 nm the mismatches is smaller than 0.4 dB with pump powers of 100 mW and 200 mW. This changes to 2.0 dB for 300 mW of pump powers. For 14 m of active fibre the largest mismatches are also mainly present at the lower wavelengths. For 1270 nm a maximum mismatch of 3.2 dB is present for 100 mW. In the wavelength range between 1300 nm and 1330 nm the mismatches has a maximum of 1.0 dB for 100 mW of pump power. These large mismatches at low wavelengths can be explained mainly by differences in background loss and coupling losses. As mentioned in section 4.2 deviations are introduced by compensating for losses of the amplifier set-up to powers at the fibre terminals. The inaccuracy of the measurement method for signal gain and pump power also introduces deviations between simulated and experimental results.

For simulations in the small signal region, the numerical error of the solver used by the model starts playing a role. This is best seen on the right side of figure 4.3.2, at longer wavelengths a ripple is present which finally results in large gain steps. This numerical error accumulates over fibre length. The error influence becomes worse at higher wavelengths caused by the high fibre attenuation in this region. This results in relative small signal powers in comparison with the accumulated numerical error. With 14 m of fibre, the accumulation of the numerical error leads to unacceptable errors at the higher wavelengths, leaps in signal gain up to 6 dB are present.

For moderate signal powers the numerical error is not a problem any more as shown in figure 4.3.3. The mismatch is highest in the low wavelength region. For 7 m of active fibre the maximum mismatch at 1270 nm is 2.9 dB and for 14 m of fibre it is 3.3 dB both for 300 mW of pump power.

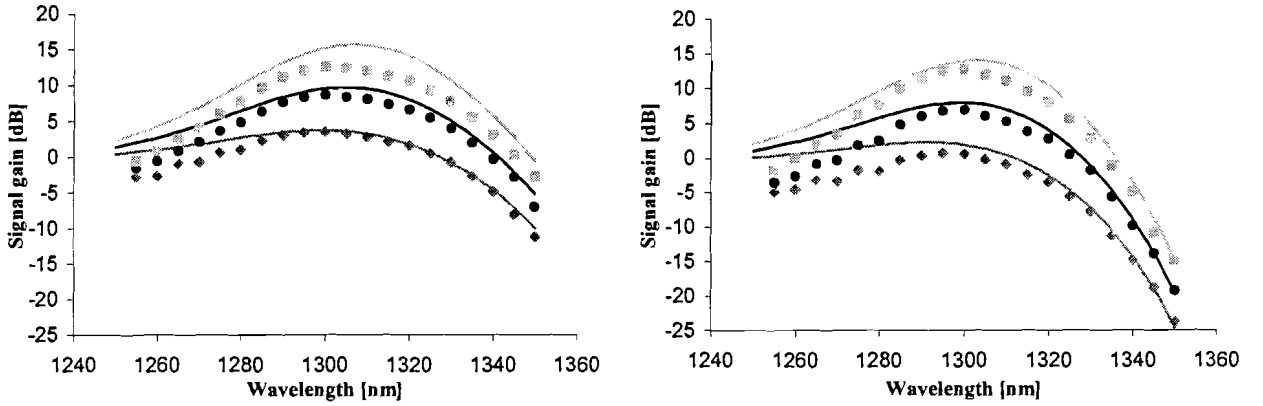

Figure 4.3.3 Gain spectrum for co-propagating pump with 100 mW (◆), 200 mW (●) and 300 mW (▒) of pump power. Signal power is –20 dBm. Left side is 7 m and right side 14 m of fibre. Solid lines represent simulated and markers experimental values.

For 7 m of fibre the match at small and moderate pump between signal gain profiles is better. In the wavelength range of 1300 nm and 1330 nm the maximum mismatch is 1.1 dB for 7 m, for 300 mW of pump power a maximum mismatch of 2.8 dB at 1330 nm is present. For 14 m of fibre and the mismatch stays under 1.3 dB in the 1300-1330 nm ranges, except for 300 mW of pump power, the mismatch is 2.0 dB at 1330 nm.

The tunable laser source used in the measurement to generate the input signal cannot generate a constant large signal power over the spectral range as used in the previous discussion. For this no signal gain spectra are used to validate the model in the large signal region.

At high pump power the gain profiles are equally shaped but the measured gain has a tendency to saturate. This effect is almost completely absent in the simulation. This is visualised by presenting the signal gain versus the pump power as shown in figure 4.3.4 at a signal wavelength of 1310 nm and signal power of –10 dBm.

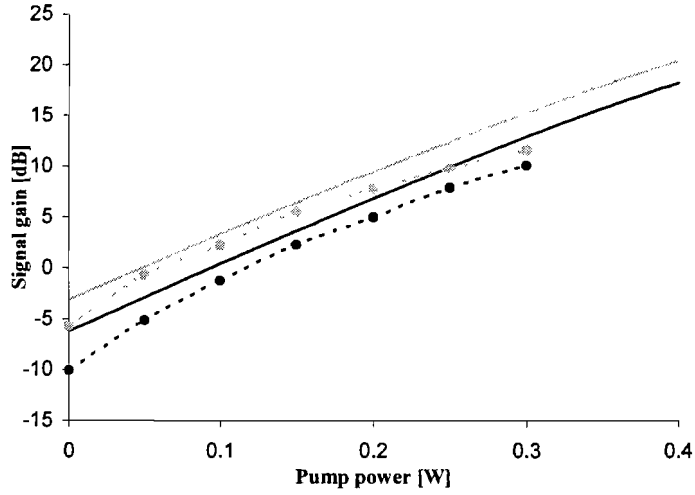

Figure 4.3.4 Gain versus pump power for co-propagating set-up. Solid lines represent simulated and dashed lines experimental values. Active fibre length 7 m (grey) and 14 m (black), signal wavelength 1310 nm and signal power -10 dBm.

A mismatch is present in the case when no pump power is applied. Correcting for deviations in background loss will reduce this mismatch. At moderate pump powers (150 mW) there is a reasonable match, a difference of 1.4 dB for 14 m and 1.0 dB for 7 m of active fibre. For 300 mW this values are increased to respectively 3.1 dB and 3.7 dB. The signal gain of the PDF module is saturated at lower pump powers and saturates stronger. The simulated signal gain shows an almost constant slope and only at the high pump powers the slope decreases somewhat. The signal gain is also saturated by high signal powers as shown in figure 4.3.5 where the signal gain is plotted versus the signal power for different pump power values.

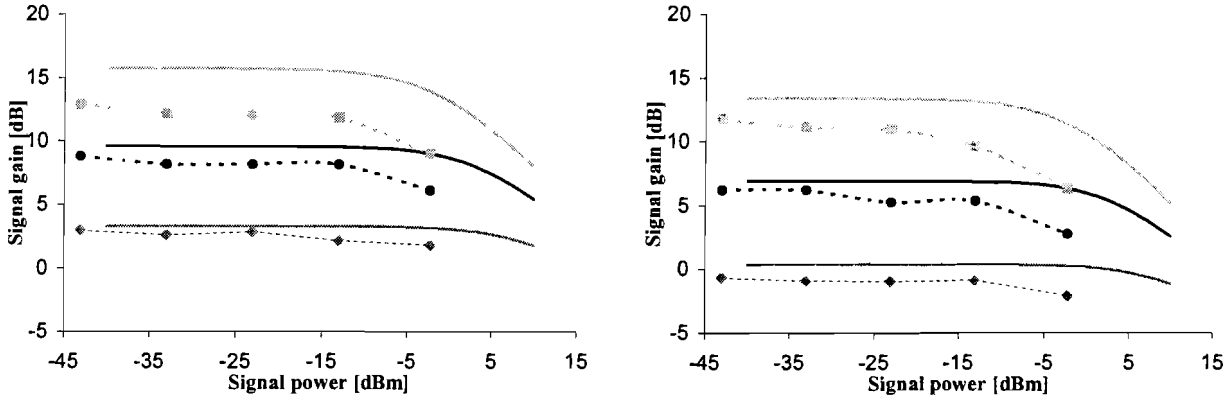

Figure 4.3.5 Gain versus signal power for co-propagating pump with 100 mW (◆), 200 mW (●) and 300 mW (■) of pump power. Signal wavelength is 1310 nm. Left side is 7 m and right side 14 m of fibre. Solid lines represent simulated and dashed lines experimental values.

For small signal powers the gain remains constant but decreases at high signal powers. For high pump powers this effect is stronger present, in addition the signal gain saturation starts for smaller signal powers. The gain mismatch for small and moderate pump powers is still on a small scale but becomes for high powers unacceptable. The point where the gain drops –3dB are for 300 mW of pump power and 7 m of fibre –6.0 dBm when measured and +1.4 dBm when simulated. For 14 m of fibre these values are respectively –10.9 dBm and +1.3 dBm.

4.4 Counter-propagating pump scheme

In this section a similar discussion as in the preceding paragraph follows, only now for the situation of a counter-propagating pump. In figure 4.4.1 the small signal gain spectra for 7 m and 14 m of fibre are shown.

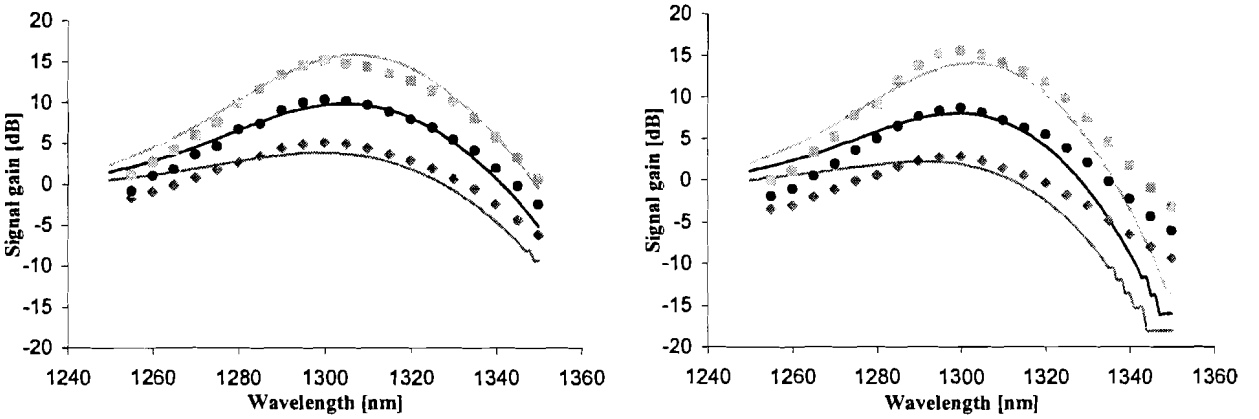

Figure 4.4.1 Gain spectrum for counter-propagating pump with 100 mW (◆), 200 mW (●) and 300 mW (■) of pump power. Signal power is –40 dBm. Left side is 7 m and right side 14 m of fibre. Solid lines simulated and markers experimental values.

The shapes of the simulated gain profiles for the short active fibre are in good agreement with the measured small signal spectra. The mismatch at small wavelengths can be explained mainly as a result of the difference in intrinsic loss, the rest of the mismatch can be explained by the same causes as mentioned in section 4.3. In the wavelength range 1300-1330 nm the maximum mismatch is 0.7 dB, except for 300 mW of pump power, then the mismatch has a maximum of 1.5 dB. For 14 m of fibre the mismatch is smaller then 0.9 dB except for 300 mW of pump power, then the mismatch is 1.6 dB.

The large deviation between experimental and simulated results at the higher wavelengths is caused by the combination of increased fibre loss and the amplified spontaneous emission (ASE) in the measured output spectrum. The enlarged fibre length causes for additive signal attenuation,

especially for the higher wavelengths. At wavelengths around 1330 nm the ASE power becomes comparable to the signal power. At even higher wavelengths the ASE power suppresses the signal power, from that point on it is no longer possible to discriminate signal power from the ASE power. The calculated signal gain is no longer valid. For 14 m of fibre the accumulation of the numerical error leads to unacceptable errors in the calculated gain, as was also the case in section 4.3.

Figure 4.4.2 shows the signal gain spectrum for a signal power of –20 dBm with different applied pump powers.

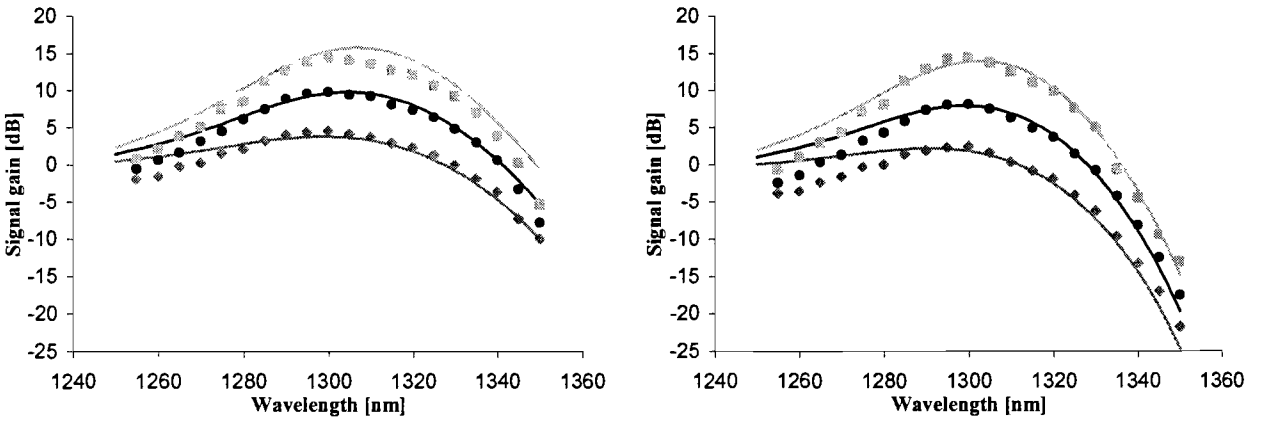

Figure 4.4.2 Gain spectrum for counter-propagating pump with 100 mW (◆), 200 mW (●) and 300 mW (■) of pump power. Signal power is –20 dBm. Left side is 7 m and right side 14 m of fibre. Solid lines represents simulated and markers experimental values.

For higher signal powers the ASE no longer suppresses the signal, the substantial mismatch at the higher wavelengths is absent. A good overlap between the measured and simulated gain profiles is present, for all pump powers. Also the mutual placement of the gain profiles agrees. For 7 m of doped fibre the maximum mismatch in the 1300-1330 nm wavelength region is smaller than 0.9 dB, except for 300 mW of pump power, then this value becomes 1.6 dB. For 14 m of fibre the maximum mismatch in this region is 1.1 dB for all pump powers. Again a mismatch occurs for the smaller wavelengths, at 1270 nm it has a maximum of 2.0 dB for 7 m of active fibre. This is mainly caused by differences in intrinsic fibre loss, the mismatch increases to 2.6 dB for 14 m of fibre length.

The signal gain is plotted versus pump power in figure 4.4.3 to examine gain saturation caused by pump power. For low and moderate pump powers the simulated and measured results are in good agreement. For 150 mW of pump power the mismatch is 0.2 dB for both fibre lengths. At high

pump powers (300 mW) this changes to 1.0 dB for 14 m and 2.2 dB for 7 m of active fibre. The saturation of the simulated active fibre is less present and starts at even higher pump powers.

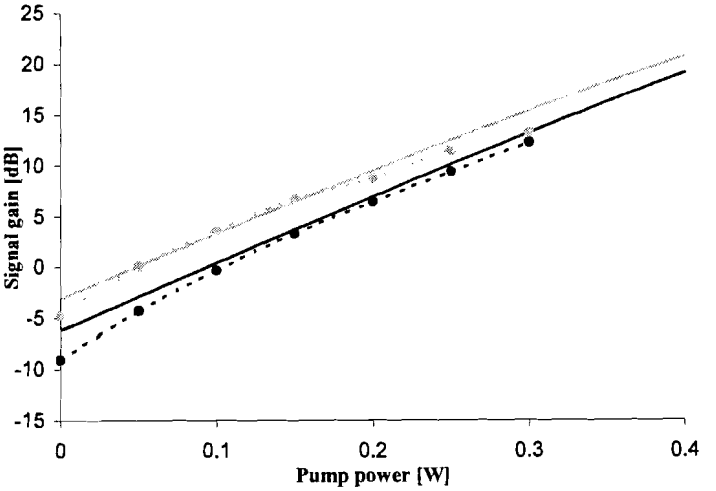

Figure 4.4.3 Gain versus pump power for counter-propagating set-up. Solid lines represent simulated and dashed lines experimental values. Active fibre length 7 m (grey) and 14 m (black), signal wavelength 1310 nm and signal power -10 dBm.

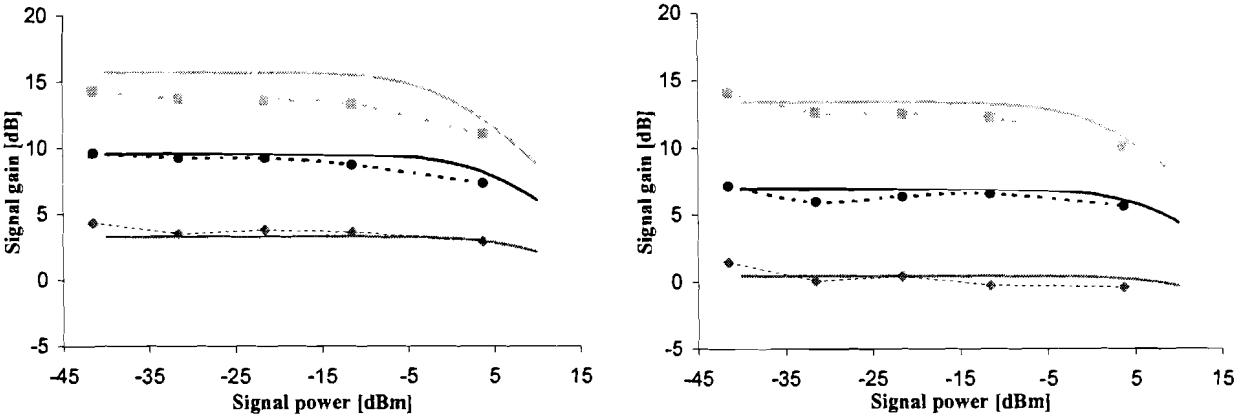

Figure 4.4.4 Gain versus signal power for counter-propagating pump with 100 mW (◆), 200 mW (●) and 300 mW (▲) of pump power. Signal wavelength is 1310 nm. Left side is 7 m and right side 14 m of fibre. Solid lines represent simulated and dashed lines experimental values.

As mentioned in the co-propagating pump section, the amplifier gain will also saturate as a result of large signal powers. In figure 4.4.4 the signal gain is plotted versus signal power for various pump powers. The signal power where the gain has dropped –3 dB is for 7 m of fibre 1.8 dBm when measured and 1.9 dBm when simulated. For 14 m of fibre these values are –3.1 dBm respectively +4.9 dBm. For low and moderate pump power the simulated and measured results are in agreement. High signal powers saturate the amplifier, especially at high pump powers. Again this effect is more

present in the experimental PDF module. At high pump powers the match stays reasonable for the situation with 14 m of fibre. For the short fibre length the placement of the signal gain curves differs seriously.

4.5 Simulated output spectra

A typical output spectrum from simulation data is depicted on the left side of figure 4.5, the right side shows a measured spectrum. Amplified spontaneous emission and signal power are both shown in the figure.

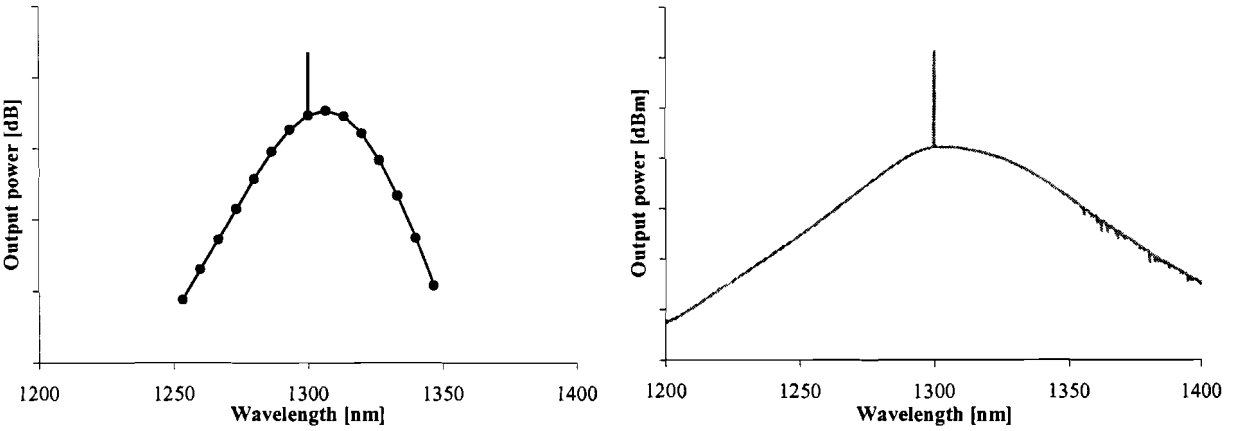

Figure 4.5 Typical simulated (left side) and measured (right side) output spectra, ASE and signal power are both shown.

When using the measurement data to determine the amplifier noise figure to validate the noise figure simulation several difficulties are encountered. The model as mentioned in chapter 3 assumes a shot-noise limited source for noise figure simulations. The laser source used in the measurements is not shot-noise limited but also produces spontaneous emission that is amplified by the PDFA. So the ASE measured at the output is not merely the ASE generated by the PDFA.
Because of the high intrinsic fibre loss the detection limit of the OSA becomes a problem when small signals are concerned. The detection limit becomes a problem even more when long fibre lengths are used in the amplifier set-up.

To determine the signal-to-noise ratio both power contributions have to be known. The ASE power is also present at the signal wavelength and distorts the measured signal power. All this contributes to an inaccurate noise figure when determined from the measurement data and it is not possible to validate the simulated noise figure derived from the model.

Chapter 5 presents more simulation results. A section is dedicated to noise figure simulations, the influence of pumping schemes and fibre length on noise figure is examined. Experimental results are presented in chapter 6. A more detailed treatment of noise figure measurements and difficulties follows in section 6.7.

4.6 Discussion

The first problem encountered by validation of the PDFA model is the difference in set-up. The model consists of only a active fibre where a practical amplifier is build up out of a compound mix of components like wavelength selective couplers, isolators and all kinds of connections between different kind of fibre types. The compensation of losses of the amplifier to powers at the fibre terminals is not without problems. This process introduces deviations in the simulation conditions. For the co-propagating pump scheme an uncertainty of around ± 0.7 dB is expected for the input signal. Mainly caused by the wavelength dependency of the WDM coupler. For the output signal the uncertainty is reduced to ± 0.4 dB. When the amplifier is counter-pumped, these values change from input to output and vice versa. No compensation in pump power is necessary, in the measurement set-up the pump power is already defined at the input of the PDF module.

The measurements on an amplifier configuration are performed as complete sets before a different amplifier configuration is being measured. This is done to prevent coupling inaccuracies introduced by changing pump scheme or fibre length. Expected inaccuracy for the output power is ± 0.2 dB caused by the OSA. For the input power this is ± 0.5 dB caused by a combination of uncertainties from laser source and optical attenuator and the OSA inaccuracy. For the total pump power coupled into the PDF module an inaccuracy of ± 0.4 dB is expected, caused by inaccuracies of the pump power tap point ratio and power meter, also the stability of pump source power over time introduces inaccuracies. For signal powers this is a minor problem compared to uncertainties in pump powers values. For instance, a measured optical pump power of 25 dBm ± 0,4 dB can introduce a worst-case deviation in pump power of 50 mW for simulation conditions.

Compensation of coupling losses and mode mismatches, caused by different fibre types with different core diameters is a problem. This can also be linked to the situation with two PDF modules in contrast with just one module. It is difficult to discriminate between background loss and coupling losses, complicating the translation from experimental set-up to simulation conditions. When applying no pump power, there is already a mismatch between measured loss and simulated

loss. This mismatch can be explained mainly by a combination of a too small value chosen for the background loss of the fibre and simulating without taking any coupling and splicing losses into account.

The mismatch, in the unpumped situation, starts to decrease at higher wavelengths. The intrinsic losses are assumed to be constant over wavelength, so probably a wavelength dependent factor is playing a role. This factor could be a deviation caused by the missing excited-state cross-section data. General inaccuracies in the experimental acquired cross-section data can also play a role. An inaccuracy in the GSA cross-section data would introduce mismatches mainly at the higher wavelengths, also when no pump power is applied to the active fibre.

For the small signal simulation, the numerical error of the model-solver starts playing a role. If the propagation equations (3.13) – (3.14) are integrated in the forward direction, a guess must be made for the powers of the counter-propagating beams at the fibre input end. A Newton-iteration technique is used to make a new guess solution before each integration. The full set of equations is integrated over and over again until the solution of all equations stabilises. The number of iterations required depends on the specific conditions of the simulation and the initial guess that is used. This error accumulates over fibre length. The error influence becomes worse at higher wavelengths caused by the high fibre attenuation in this region. This results in relative small signal powers in comparison with the numerical error. For relatively short fibre lengths the error stays acceptable, but for long fibre lengths the error quickly accumulates to unacceptable values.

In the future, when experimental results from a bi-directional pump configuration become available, it is recommended to validate the fibre model in a bi-directional pump scheme. Impressed is on acquiring exact excited-state cross-section data, cancelling out the inaccuracy present at this moment. A precise method to determine the PDF-modules background loss separated from any coupling and splicing losses is required. The coupling losses should also be determined exactly. This is necessary to make an accurate translation between experimental and simulated conditions.

4.7 Conclusions

Two important factors, which make it difficult to validate the model, are the inaccuracies introduced by the measurements and the uncertainties introduced when transforming experimental data to suite simulation conditions. Limiting the components and the connections used in the amplifier will increase accuracy. Another major problem is the distinction of intrinsic fibre loss into background

loss and coupling losses and the exact determination of these losses. Further and more accurate measurements are necessary to determine these parameters. From this it is concluded that a correct model can still result in invalid outcome caused by inaccurate simulations conditions.
The measurement method used to determine signal gain is not suitable to determine accurate amplifier noise figures. Validating the noise figure section of the model is not possible with the measurement data.

In general the model outcome satisfies experimental results. Only for the lower signal wavelength the model is not valid. This region increases to higher wavelengths at increasing fibre length. But around 1300 nm the model stays valid. A great part of the mismatch is caused by the difference in intrinsic loss of the fibre. Additional background loss would compensate for a great part of the mismatch resulting in a general better overlap. In general, care must be taken in determining the background loss (dB/m) of the fibre. A small error in background loss can quickly accumulate into an unacceptable error when large fibre lengths are used in the amplifier set-up.

The PDF module signal gain saturates earlier and heavier by large signal and pump powers compared to simulation results of the active fibre. A process limiting signal gain, conditioned to the available power in the active fibre core, can be playing a role. The model uses some essential transitions between simplified energy levels to calculate population densities as depicted in figure 3.5. For instance pump ESA and co-operative upconversion are neglected as well as possible non-radiative transitions between the various levels. These transitions shorten emission lifetime and limit the amplifiers signal gain.

Input signal powers of -40 dBm into the active fibre are around the limit for useful results when moderate fibre lengths are concerned. At long fibre lengths this will already result in substantial numerical errors at the higher wavelengths.

5 Simulations

5.1 Introduction

In this chapter some more simulation results are presented. This section is divided into three sections. In the first section the influence of some important fibre parameters on the simulation results are studied in a parameter-sensitivity analysis. In chapter 4 some mismatches where observed between results from simulations and experiments. Part of the mismatch is explained as caused by deviations in fibre parameters. To validate this assumption it is necessary to examine the influence of some fibre parameters and simulation conditions. These parameters all act upon each other, influencing the amplifier behaviour.

The next section is dedicated to the bi-directionally pumped amplifier. It was not possible to realise a practical bi-directional pumped amplifier, so the simulation results of this configuration cannot be validated with measurement data.

In the third section results from noise figure simulations are presented. The influence of signal power and pump power on the amplifier noise behaviour is examined. This is done for a co-, counter- and bi-directional pumping scheme.

5.2 Fibre parameter sensitivity analysis

5.2.1 Cut-off wavelength and numerical aperture

The cut-off wavelength is an important fibre parameter, also because it is closely related to the fibre core diameter and NA. There is an optimum value for the cut-off wavelength. The mode profiles of pump and signal differ because of the different wavelengths. If the cut-off wavelength is decreased, the optical intensities will increase as the modes are confined to a smaller area. Furthermore, the pump and signal modes will show better overlap. This means that the fibre is being less under-pumped in the section close to the cladding where the signal power is still quite strong. But if the cut-off wavelength is increased too far, a considerable part of the optical power will propagate in the undoped cladding and will not contribute to amplification.

The influence of NA signal gain is shown on the left side of figure 5.2.2 for various NA values. A co-propagating pump scheme with 7 m of active fibre is used. A total of 300 mW of pump power is coupled into the fibre and the input signal power is –30 dBm. The PDF module is specified with a NA of 0.182, and in the simulation the NA is varied around that value.

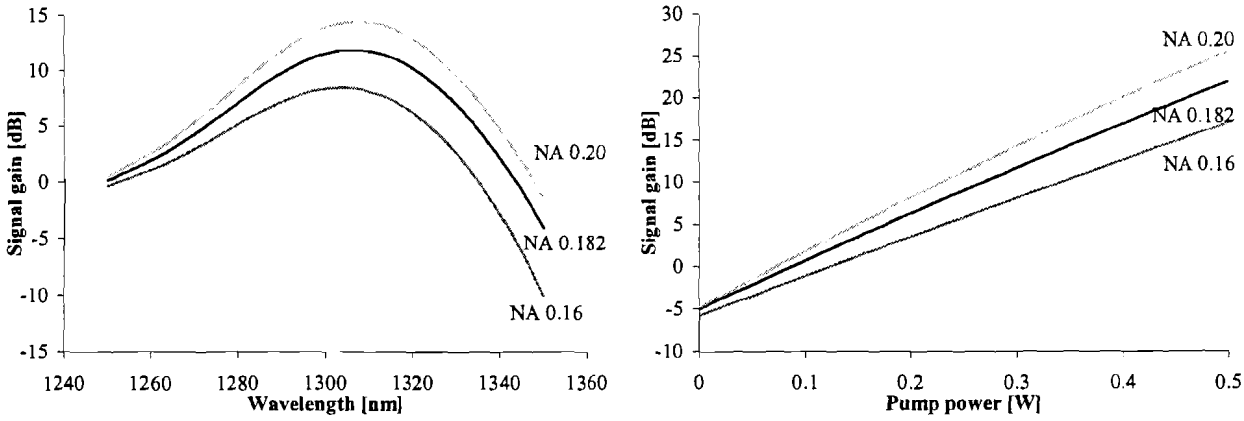

Figure 5.2.2 Left side: Signal gain versus wavelength for different NA values, applied pump power is 300 mW. Right side: Signal gain (1310 nm) versus pump power for different NA values. The 7 m of active fibre is co-directional pumped.

The importance of a well-chosen NA becomes clear in the signal gain spectrum. A small change in NA results in large differences in signal gain, especially in the important wavelength region around 1300 nm. The right side of the same figure shows a plot of the signal gain versus pump power coupled into the fibre, again with the same variations of NA. Already small pump powers result in substantial differences in signal gain between the different NA-type fibres. This becomes more evident when comparing the pump powers involved for where the fibre starts to amplify. The high NA-fibre starts to amplify at much smaller pump powers compared to the low NA-type fibre.
The NA is related to the refractive index difference of core and cladding of the fibre by:

$$NA = \sqrt{n_{core}^2 - n_{clad}^2} \qquad [\mathrm{m}^{-1}] \tag{5.1}$$

This means that the used host glass material limits the choice in NA. The signal gain increases with increasing NA [1]. From (3.1) and (3.5) it follows that the core radius decreases, while the normalised frequency remains the same. Using this result in (3.4), it is found that the optical intensities increase with increasing NA. The shape of the mode fields does not change but are only confined to a smaller radius, as there are no counterbalancing effects. Pumping efficiency is increased and the low quantum efficiency is partly compensated [2]. Limitations to this are the available pump power and the fact that noise (ASE) is generated, which also consumes pump power. Thus the gain flattens for high NA values. The NA is also limited cause a too high NA will lead to unpractical small core diameters and subsequent coupling difficulties.

5.2.3 Fibre length

On the left side of figure 5.2.3 the signal power evolution along the fibre is shown. In the simulation the powers along the fibre distance are calculated, this is done for different co-propagating pump powers. The optimum fibre length is closely related to the available pump power. The more power available, the longer the fibre has to be to benefit from the extra power. For low pump powers the maximum signal gain is reached at a shorter fibre length, compared to the situation when high pump power is applied to the active fibre.

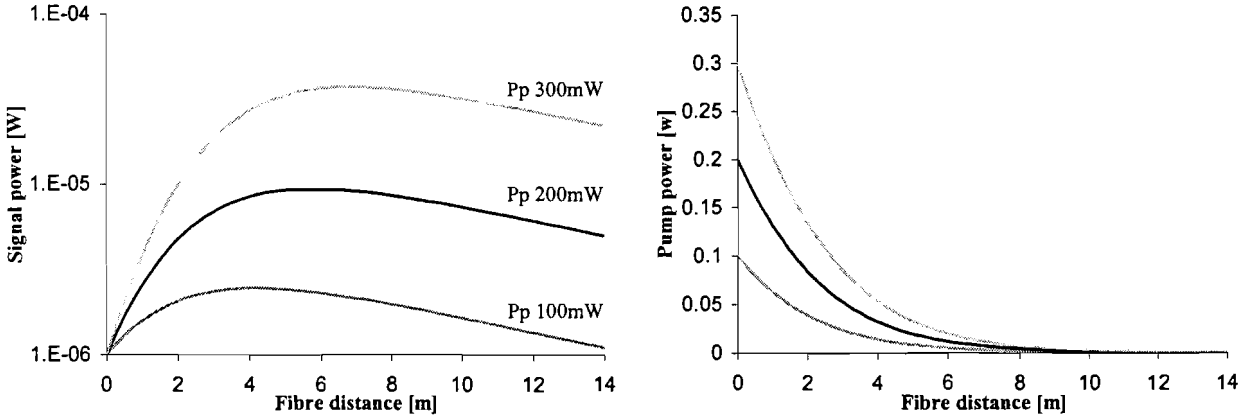

Figure 5.2.3 Left side: Signal power (1310nm) versus fibre distance. Right side: Pump power versus fibre distance. Both co-directional pumped with 100 mW, 200 mW and 300 mW of pump power.

The right side of the figure shows the pump power evolution when travelling through the fibre. Higher pump powers require more fibre length to be totally absorbed. In addition, when the fibre is relatively short there is also a change of residual pump power at the fibre end. But for each value of pump power there is an optimum. If the fibre is too long, the signal will be attenuated in the last section due to the increase in background loss and ground state absorption, at the unpumped part of the fibre signal photons can be absorbed by ions in the ground state.

5.2.4 Doping concentration and profile

Signal gain spectra are displayed for different peak doping concentrations in figure 5.2.4. In all cases a uniformly doped profile is used for the active fibre.

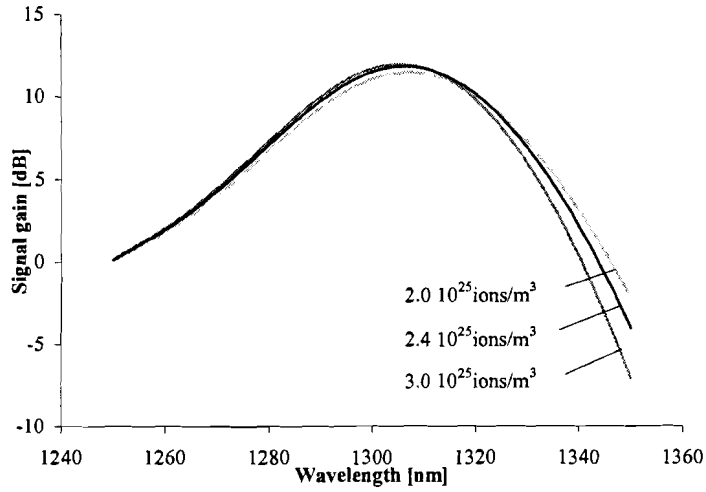

Figure 5.2.4 Signal gain spectrum for different peak doping concentrations. The7 m of fibre length, uniformly doped, is co-directional pumped with 300 mW of pump power.

Two noteworthy effects are observed. To some extent the signal gain values alter, a higher concentration of praseodymium results in higher signal gain. But this effect is also associated with the signal wavelength. For small wavelengths the change in doping concentration has no major influence on signal gain. But at somewhat higher wavelength the signal gain profiles are shifted and reshaped. So for higher doping concentrations the signal gain increases around 1300 nm, but also narrows the signal gain region. A low doping concentration yields to a broadened amplifier bandwidth.

In principle a high doping concentration is preferred leading to higher signal gain values and short fibre lengths. This would also result in reduced fibre background losses. Unfortunately the use of high doping concentrations is severely limited. As mentioned in section 3.3, all kinds of processes related to high doping concentrations take place, like for instance co-operative upconversion and cross-relaxation. This decreases emission lifetime and reduces amplifier efficiency [3,4].

This report considers fibres having a uniform doping distribution. It is also possible to confine the doping closer to the fibre axis. If the doping is mainly centred on the axis core, the fibre gain efficiency can be further increased caused by the higher population inversion. This results in a high intensity of the pump and signal modes in the proximity of the fibre axis [5].

5.2.5 Signal excited-state absorption

Although incorporated in the fibre amplifier model no signal excited-state absorption data are available for the PDF module. For numerical reasons a very small constant value of 10^{-30} m^2 is selected for the ESA cross-section, so no noticeable influence on amplifier behaviour is present. Figure 5.2.5 shows the signal gain spectrum of the active fibre for different ESA cross-sections. In four cases the ESA cross-section is a constant value of 10^{-30}, 10^{-27}, 10^{-26} and 10^{-25} m^2.

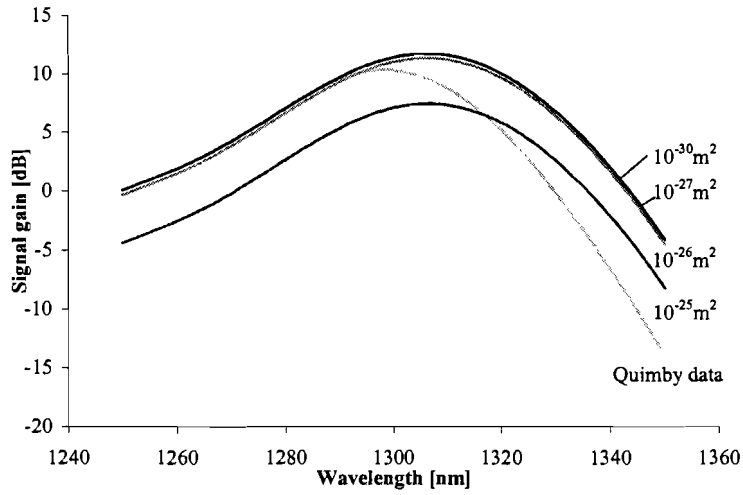

Figure 5.2.5 Signal gain spectra for various ESA cross-section data. Co-directional pumped (300 mW), fibre with 7 m of doped fibre length.

An ESA cross-section at the signal wavelength reported by Quimby and Zheng [6] is included as input for the praseodymium-doped fibre amplifier model. For a constant ESA cross-section value of 10^{-22} still no influence in signal gain is noticed, the gain profile remains the same for the case of an ESA value of 10^{-30} m^2. Further increase of the ESA cross-section results in a downward shifted gain profile. The profile shifts down to lower signal gain values for almost all wavelengths. At higher wavelengths the reduction in signal gain is smaller. This is caused by the fact that the available signal gain in that region is relatively small, so the influence of the excited-state absorption will also be reduced.

A more realistic ESA cross-section is that of Quimby and Zheng. The cross-section values are negligible for wavelengths below 1300 nm, the peak value is located around 1400 nm. So for low wavelengths the signal gain is not altered, but around 1300 nm the reduction in signal gain is substantial. The signal gain decreases even further at higher wavelengths.

5.2.6 Fibre background loss

The background loss (α) is a sensitive parameter; an error will quickly accumulate for long fibre lengths. In the simulations performed in the preceding chapter a too small value was chosen. In figure 5.2.6 the signal gain spectrum is plotted for different background losses for 300 mW of co-propagating pump power. This is also done for a passive fibre when no pump power is applied, in this case the term signal loss spectrum is more appropriate.

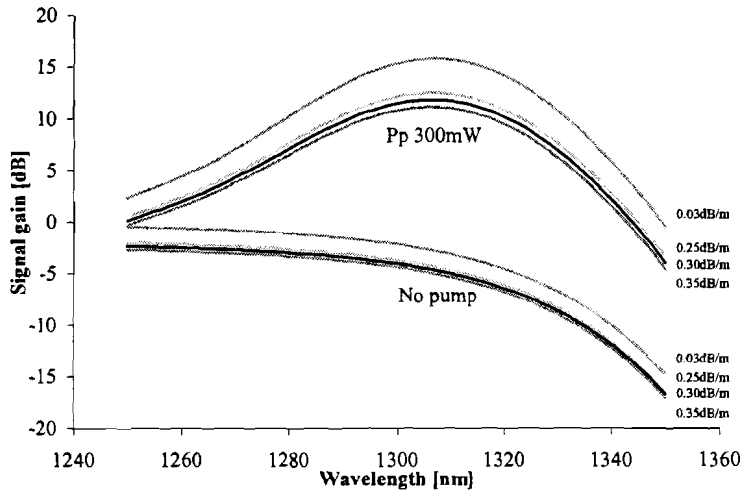

Figure 5.2.6 Signal gain versus wavelength for different values of background loss. This is done for 300 mW of co-directional pump power and for the case when no pump power is applied. Signal power –30 dBm and the active fibre length is 7 m.

A relatively short fibre length of 7 m is used. A small change in background loss introduces already a substantial difference in loss when no pump power is applied. The signal loss difference at a wavelength of 1310 nm for α values of 0.25 dB/m and 0.35 dB/m is 0.7 dB, exactly as expected for a Δα of 0.1 dB and 7 m of active fibre. When the amplifier is being pumped the difference in signal gain increases considerably. At a signal wavelength of 1310 nm the difference in gain is 1.4 dB for α values of 0.25 dB/m and 0.35 dB/m. As long as the fibre gain is unsaturated this gain difference caused by background loss variations increases with pump power.

5.2.7 Emission lifetime

The praseodymium-doped fibre amplifier model also neglects non-radiative transitions. These transitions reduce the emission lifetime. Figure 5.2.7 is used to examine the effect of changes in emission lifetime on signal gain. Depicted is the signal gain spectrum for different lifetime values, for 7 m of co-propagated pumped fibre.

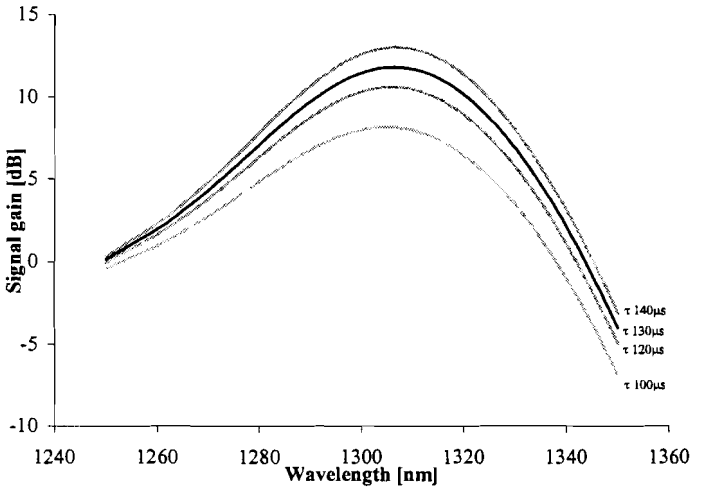

Figure 5.2.7 Signal gain versus wavelength for different lifetime values. Co-propagating pump scheme with 300 mW of pump power and 7 m of active fibre.

The emission lifetime (τ) of the PDF module is specified with a value of 130 μs. The emission lifetime is varied around this value. A longer lifetime results in higher signal gain in the entire wavelength region. Subsequently, a shortened lifetime yields in smaller signal gain. Under these simulation conditions and lifetimes between 100-140 μs the differences in gain are linear related with a coefficient of 0.12 dB/μs at a wavelength of 1300 nm. The signal emission is most probable around a wavelength of 1300 nm, so variations in emission lifetime will exert maximum influence on the signal gain in this region.

5.2.8 Discussion

In this section a fibre parameter analysis is performed using the praseodymium-doped fibre model. Most parameter deviations demonstrate a substantial influence on signal gain. So extreme care must be taken in determining the exact values of these parameters. Just small variations in background loss, NA or emission lifetime are needed to introduce sizeable changes in signal gain. Parameters like doping concentration and profile also influence the signal gain spectrum shape. This also applies for an actual ESA cross-section, which normally decreases signal gain starting at signal wavelengths around 1300 nm. The interaction between some parameters is also of importance especially in fibre design. For instance the optimum fibre length is closely related to available pump power, background loss and doping concentration. The NA greatly influences pump power efficiency but the freedom in NA value is also limited by material parameters as practical refractive index differences and core diameters. Furthermore the connection of the doped-fibre to another fibre must be possible with low insertion loss.

5.3 Bi-directional pump scheme

5.3.1 Simulation results

Simulations are performed on a bi-directional pump configuration. In figure 5.3.1 signal gain is plotted versus pump power, this is the overall fibre gain without compensation for fibre losses. The pump power is the total power applied, equally divided on both sides. For a small signal power there is no strong saturation. The shortest fibre length results in the highest gain. Beyond a certain pump power value this changes in benefit of the longer fibre. The higher fibre loss is then compensated and the extra gain becomes available when applying even more pump power. The amplifier saturates at lower pump power and stronger for large signal powers. The extra length of doped fibre does not result in higher gain values for large signal powers.

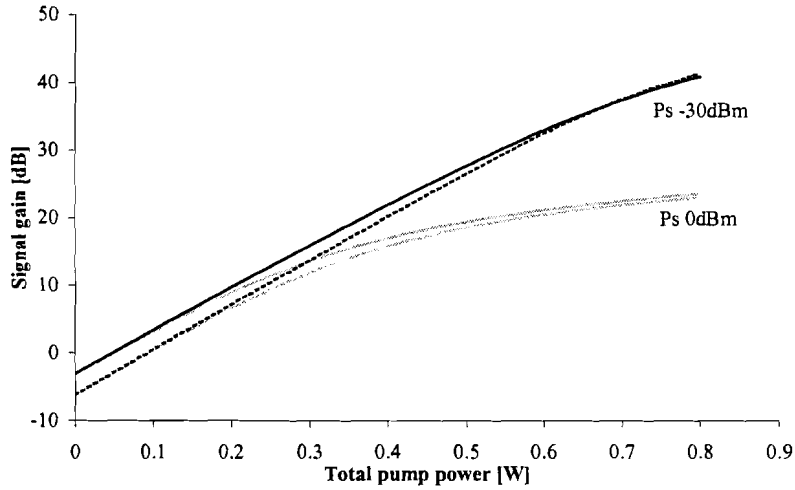

Figure 5.3.1 Signal gain versus total pump power for signal powers of –30 dBm (black) and 0 dBm (grey) at 1310 nm. Total fibre length is 14 m (dashed) and 7 m (solid).

The signal gain spectra are shown in figure 5.3.2 for different pump power values. In all situations the short fibre length results in higher signal gain. But at higher pump power the difference in signal gain decreases. Losses introduced by the extra fibre length are almost completely compensated around 1300 nm. The higher wavelengths still suffer from extra fibre losses. The low pump power efficiency at these wavelengths makes it hard to compensate for this intrinsic fibre loss. So under these conditions a short fibre length results in the highest gain and the best amplifier bandwidth.

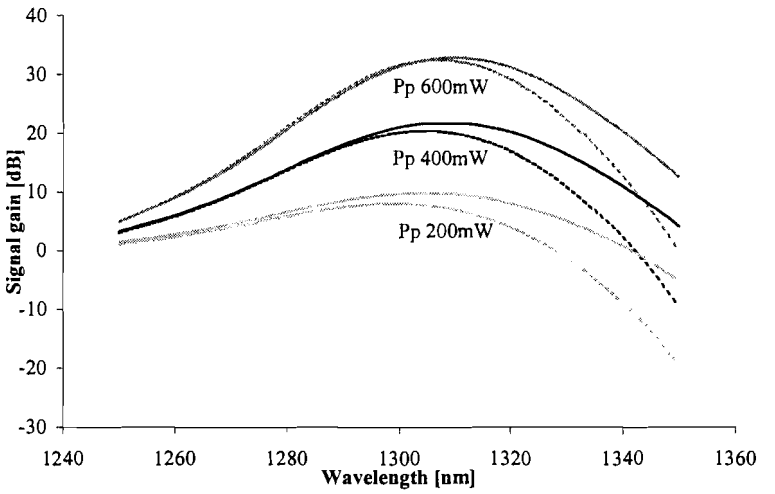

Figure 5.3.2 Signal gain versus wavelength for different pump powers. Pump power is the total amount of power applied in both directions. Signal power is –30 dBm, fibre length is 7 m (solid) and 14 m (dashed).

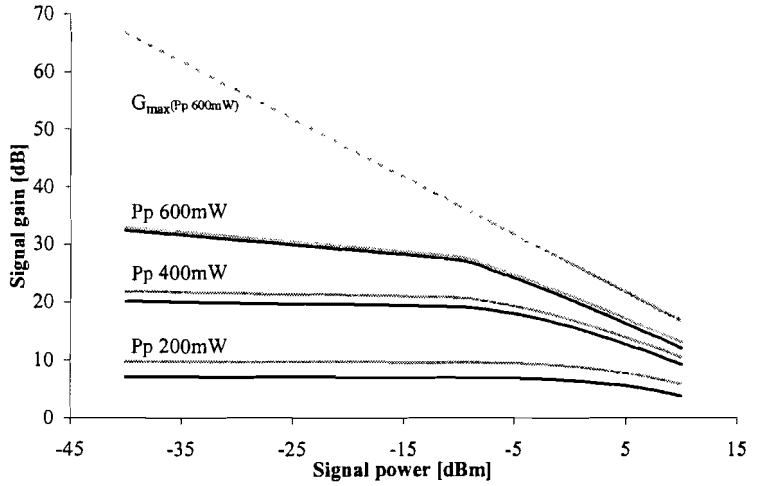

Figure 5.3.3 Signal gain versus signal power (1310 nm) for different pump power values. Grey lines represent 7 m and black lines 14 m of doped fibre.

Gain saturation caused by the signal and pump becomes more distinct in figure 5.3.3. At higher pump power the point of saturation occurs at lower signal power values. The saturation also becomes stronger. The saturation caused by the signal power is almost identical for both fibre lengths. In all cases the short fibre results in higher signal gain. But for higher pump powers the gain differences become smaller and will finally result in benefit of the long fibre length, which also appeared from figure 5.3.1.

Added in the figure is the maximum signal gain for 600 mW of pump power (λ_p 1030 nm). The theoretical limit of the gain follows from [7]:

$$G_{\max} = 10^{10} LOG\left(\frac{P_p}{P_s}\frac{\lambda_p}{\lambda_s}\right) \quad [\text{dB}] \tag{5.2}$$

In practice this limit will never be reached. Amplified spontaneous emission is generated which consumes part of the pump power.

5.3.2 Discussion

Because of the low quantum efficiency of praseodymium-doped fibre large amounts of pump power are required to overcome fibre losses and achieve substantial signal gain. With a bi-directional pumping scheme it is possible to deliver these large amounts of pump power to the active fibre. In a practical amplifier still some problems have to be solved. In the case of bi-directional pumping residual pump powers enter neither the input or output fibre. Both WDMs couple it to the other pump module. Care must be taken that residual pump powers are not too high, as the pump lasers may become unstable or even be damaged. Isolators can be placed in the pump path to protect the pump laser for this reflected pump power. The isolators used to protect the laser sources typically inhibit a high insertion loss, decreasing the coupled pump power to a large extent. The insertion loss introduced by the two necessary WDM decreases the available pump power into the fibre even further.

The bi-directional pump scheme shows a potential for high small signal gain when these practical problems are not considered. For small signals the population inversion reaches its maximum when balanced bi-directional pumped [8]. This can be clarified by the fact that a pump scheme which provides a nearly uniform pump power distribution along a doped fibre is desirable as it overcomes the problems of the reduction in PDFA gain efficiency caused by pump ESA and co-operative upconversion in the small signal range [2,9,10]. Bi-directional pumping also generates a different ASE pattern. When the fibre is sufficiently long this can result in higher small signal gains, for equal amounts of pump power compared to the co- or counter-propagating pumping schemes [11].

The long fibre length only pays off at very high pump values, also the extra fibre length does not offer any signal gain advantages when large signals are concerned. The lower intrinsic loss will result in higher powers available at the output. The lower loss at the higher signal wavelengths is

also the reason for the broader gain bandwidth for 7 m of fibre. As a consequence the short fibre is preferred in a bi-directional pumping configuration.

5.4 Noise figure simulations

5.4.1 Simulation results

All simulations are performed with no optical filter at the amplifier output, a filtered output will result in better noise performance. The performed noise figure simulations are not comparable with system applications. They are used to indicate trends in noise figure behaviour, which changes when the pumping scheme, pump and signal powers or active fibre length changes.
In figure 5.4.1 the noise figure is plotted versus signal power. This is done for a co-directional and a counter-directional pump scheme with 7 m of active fibre. The noise figure curves are plotted for different pump power values.

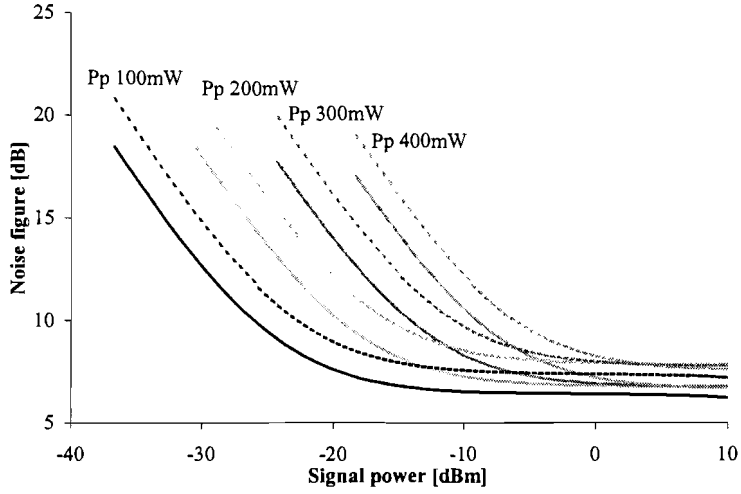

Figure 5.4.1 Noise figure versus signal power (1310 nm) for different pump powers and a fibre length of 7 m. Solid lines represents co-propagating pump and dashed lines counter-propagating pump.

The co-propagating pump scheme has a better noise performance. Under all conditions it performs better resulting in a lower noise figure compared to counter-propagated pumping. The amplifier performs best at low pump power resulting in relatively low ASE noise contributions. At high signal powers the signal is strong enough compared to the ASE resulting in high SNR at the output of the amplifier. Below a certain signal power, it will no longer influence the ASE contribution. The ASE power remains unchanged and as the signal power is further decreased the SNR at the output decreases and the noise figure increases proportionally. At these low pump powers the amplifier gain quickly saturates by the signal power resulting in an almost constant noise figure for the large

signals. When applying more power the saturation point is shifted to higher signal powers. Also the ASE contribution increases resulting in an overall worse noise figure and the point where the signal power becomes to small to influence the ASE behaviour is also shifted to higher signal powers.

Next the length is doubled resulting in 14 m of active fibre, all other conditions are left unchanged. The results are depicted in figure 5.4.2.

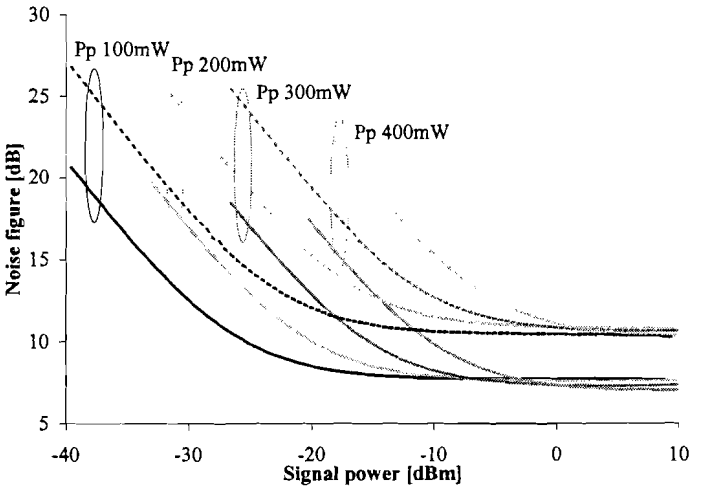

Figure 5.4.2 Noise figure versus signal power (1310 nm) for different pump powers and a fibre length of 14 m. Solid lines represents co-propagating pump and dashed lines counter-propagating pump.

The enlarged fibre introduces more background loss reducing the noise figure. The extra fibre length also introduces more available gain. Normally high pump power values are required to compensate for the extra intrinsic loss. At low pump powers the ASE benefits the most from the available gain decreasing SNR. But at high pump powers this changes, resulting in better noise figure values compared to low pump powers. The difference in noise figure as a result of pumping scheme is further increased to the disadvantage of the counter-pumped amplifier.

In figure 5.4.3 noise figure simulation results are presented for a bi-, counter- and bi-directionally pumped amplifier. The pump power values mentioned are the total powers, so for the bi-directional pump scheme half the power is applied to each pumping side. The bi-directional pumped amplifier noise figure performs better than counter-pumped and worse than co-pumped. This is expected because a bi-directional amplifier can be seen as an amplifier consisting of a co- followed by a counter-directional pumped amplifier. The figure is more suitable for comparing differences in noise figure as a result of fibre length.

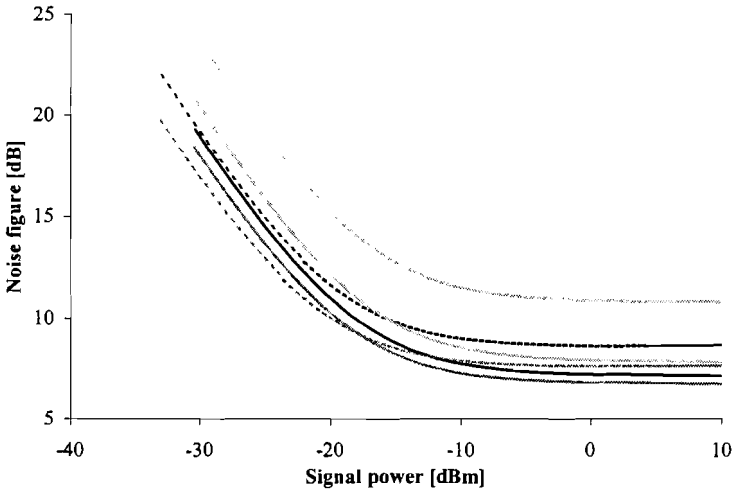

Figure 5.4.3 Noise figure versus signal power (1310 nm) for different pump schemes. Bi- (black), counter- (light grey) and co- (medium grey) directional pump scheme with 200 mW of total applied pump power. Dashed lines 14 m and solid lines 7 m of fibre.

5.4.2 Discussion

For consideration of noise in small signal gain amplifiers, the two pumping schemes co- and counter-propagating are contrasted first. This is particularly applicable to preamplifier and inline amplifier design, in terms of obtaining the lowest noise figure possible. In general, the co-propagating pump offers the lowest noise figure, considering only the doped fibre and ignoring any loss from passive components before or after the doped fibre [11].

The reason for this is that in the co-propagating configuration the portion of the fibre that the signal enters tends to be more inverted than the section by which the signal exits. Thus, the signal undergoes more gain per unit length at the beginning of the fibre than at the exit. In the counter-propagating configuration, the inverse situation is present, and the lower gain per unit length at the beginning of the fibre is equivalent to having some amount of loss for the signal before it enters the amplifier.

Any loss that the signal experiences at the beginning of the fibre will degrade the noise figure. Thus, in absence of any other effects, the co-propagating pump is preferred for obtaining a low noise figure. This argument is not as valid if the fibre is short enough. In that case, assuming that pump power is not limited, a strong enough pump will strongly invert the entire fibre and it will not matter whether the pump is co-propagating or counter-propagating.

The backward travelling ASE does not significantly alter the population of the metastable state when counter-directional pumped [12]. Loss in the passive components used in the amplifier as a

whole alters this, the input is coupled directly to the active fibre, without any intervening loss. When co-directional pumped, a WDM coupler that combines the pump and signal is placed immediately before the doped fibre. This WDM coupler has some loss at the signal wavelength and thus the noise figure is reduced by the loss experienced by the signal to the WDM.

Bi-directional pumping leads to noise figures worse than co- and better than counter-directional pumped. But bi-directionally pumping needs more passive components decreasing the noise figure. The value of the noise figure arrived from the simulation can be improved by placing a narrow band pass filter at the output of the amplifier which decreases the amount of ASE contribution.

6 Experimental results

6.1 Introduction

This chapter handles the experimental results in a more detailed manner. In chapter 4 some of these results were used to validate the model, so the comparison between measurements and simulations are emphasised. At this point the differences and similarities in the experiments caused by the pumping scheme become of more importance. The amplifier behaviour in the different signal regions also becomes of interest. So the results are discussed by comparison between co-propagating and a counter-propagating pumping. This chapter is split up in small, moderate and large signal regions. Signal powers of –40 dBm up to –30 dBm are considered as small signals. The moderate signal region is located between the small signal and large signal region. Signal powers above –30 dBm and below 0 dBm are meant. Signal powers of 0 dBm and more are considered as being large.
After that a section follows with experimental results of a special amplifier configuration, a signal double-pass configuration. By doing this, also a comparison between single- and double-pass will be possible.

6.2 Small signal region

In most of the results shown here the net fibre gain is used. This gain is not the actual overall gain measured from isolator to isolator, but the difference between the pumped and unpumped situation. By doing this, it is more convenient to draw a comparison between different doped fibre lengths, because all intrinsic fibre losses are compensated.

In figure 6.2.1 the net fibre gain is plotted versus the signal wavelength. In the lower signal wavelength range there is just a small difference in gain for co- and counter-directional pumping. At the rest of the wavelength region the counter-propagating pump leads to a better gain. For 7 m of fibre this is still a small amount, but in the case of 14 m of fibre length it is a considerable difference. Actual gain values are listed in appendix C.

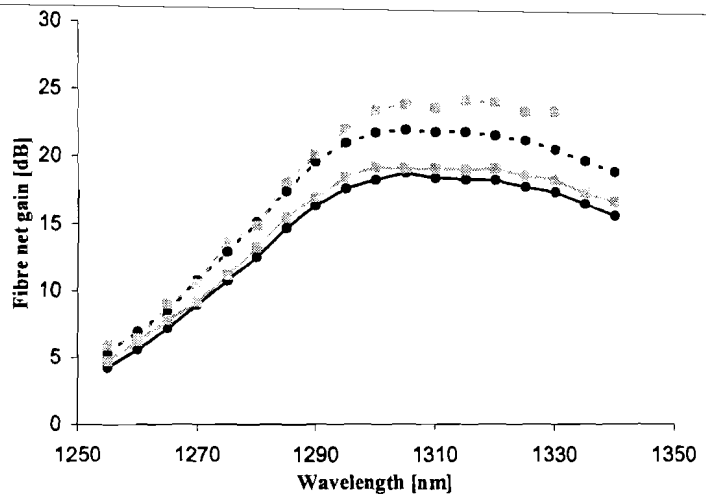

Figure 6.2.1 Fibre net gain versus signal wavelength for a signal power of –40 dBm. Pump power is 300 mW co- (●) and counter- (■) directional pumped. Solid lines represents 7 m and dashed lines 14 m of fibre.

For discussions of the amplifier bandwidth, it is more suitable to use the overall amplifier gain. This is the gain measured from input isolator to output isolator. In figure 6.2.2 this signal gain is plotted versus wavelength for both co- and counter-directional pumping. The amplifier exhibits a large region with available signal gain. Especially when the short fibre length is used. With 14 m of fibre the fibre loss increases, particularly at the higher wavelengths, resulting in a decreased gain.

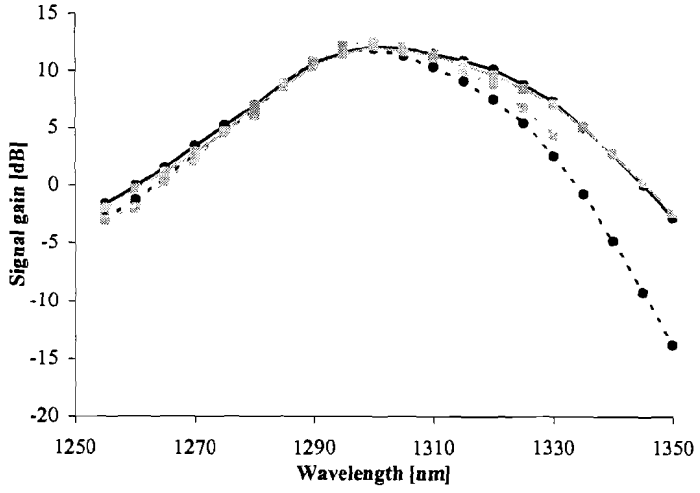

Figure 6.2.2 Small signal gain (-40 dBm) with co- (●) and counter- (■) directional pump power of 300 mW. Solid lines represents 7 m and dashed lines 14 m of doped fibre.

In table 6.2 some important characteristics extracted from figure 6.2.2 are denoted. The bandwidth (B) used in the table is the wavelength region where the maximum signal gain has dropped –3 dB.

In all situations the maximum gain is achieved at a wavelength of 1300 nm. The short fibre length results in a larger bandwidth. The bandwidth is slightly better when co-directional pumped for both lengths.

Table 6.2 Several amplifier characteristics in the small signal region.

Pump scheme	*Fibre length* [m]	λ_{Gmax} [nm]	$Gain_{max}$ [dB]	λ_{min} [nm]	λ_{max} [nm]	B_{-3dB} [nm]
Co	14	1300	11.8	1285	1316	31
Counter	14	1300	12.5	1287	1316	29
Co	7	1300	12.1	1286	1323	37
Counter	7	1300	12.1	1287	1321	34

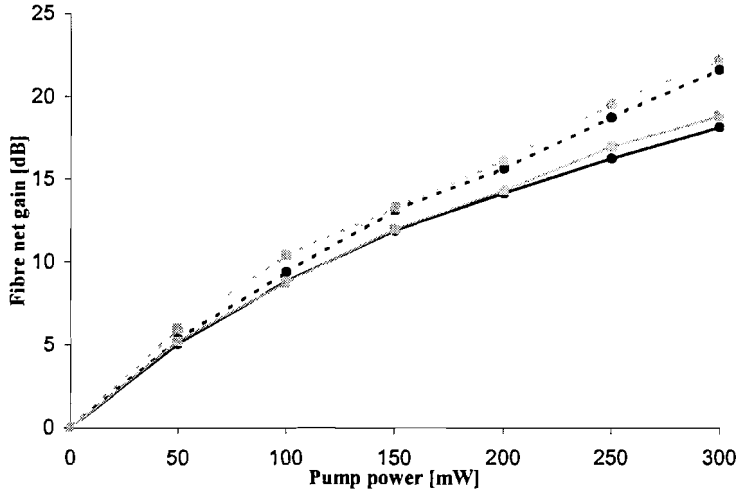

Figure 6.2.3 Small signal fibre net gain versus pump power. Signal power is –40 dBm at 1310 nm. Co- (●) and counter- (▒) directional pumped. Solid lines represents 7 m and dashed lines 14 m of fibre.

The fibre net gain is plotted versus the pump power in figure 6.2.3. For small values of pump power there is no large distinction between co- and counter-directional pumping. The slope of the gain curves represents the pump power efficiency; these are determined in a pump power region far from gain saturation. For 7 m of fibre the pump power efficiency is 0.089 dB/mW and 0.088 dB/mW for respectively a co- and counter-directional pump. For 14 m of fibre these values are respectively 0.094 dB/mW and 0.104 dB/mW.

At high pump powers the counter-pumping scheme leads to higher gain values. Also the difference between 7 m and 14 m of fibre becomes more distinct in favour of the longer fibre length. There is

no strong saturation effect present, so higher pump powers would lead to even higher gain values. This saturation effect occurs first of all at the shortest fibre length.

6.3 Moderate signal region

To get an overview of amplifier saturation as a result of signal power, the fibre net gain is plotted versus signal power in figure 6.3.1. For small signals the gain will be highest but will remain relatively constant at increasing signal power until the amplifier saturates.

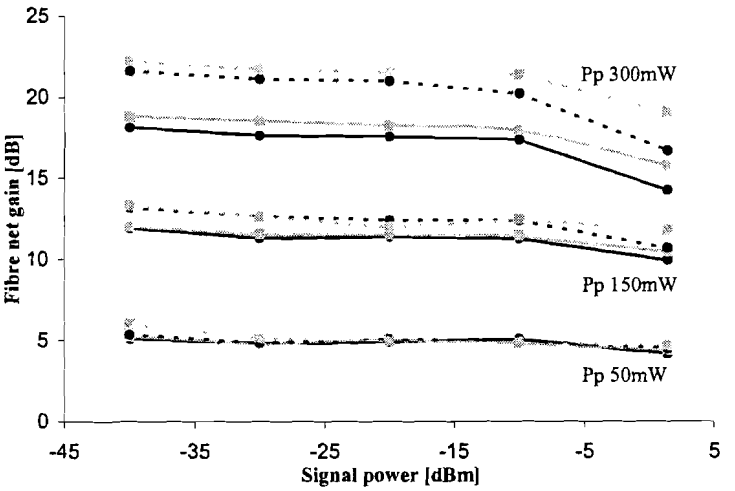

Figure 6.3.1 Fibre net gain versus signal power for different pump powers, with co- (●) and counter- (▒) propagating pump. Signal wavelength is 1310 nm, solid lines represent 7 m and dashed lines 14 m of doped-fibre.

For small pump powers, the scheme of pumping makes no distinct difference. There also is no strong gain saturation at high signal powers. For higher pump powers the gain profiles start to differentiate. In the whole signal power span, the counter-propagating scheme outperforms the co-pumping situation with higher gain values. For high signal powers there is a modest tendency for the gain to saturate. For even higher pump powers the advantages of the extra fibre length are evidently present, much more signal gain compared to the short fibre length. Applying more pump power would probably lead to an even larger gain difference between the short and long fibre. At high signal powers the gain saturation becomes stronger present. This saturation is stronger when the amplifier is co-directionally pumped.

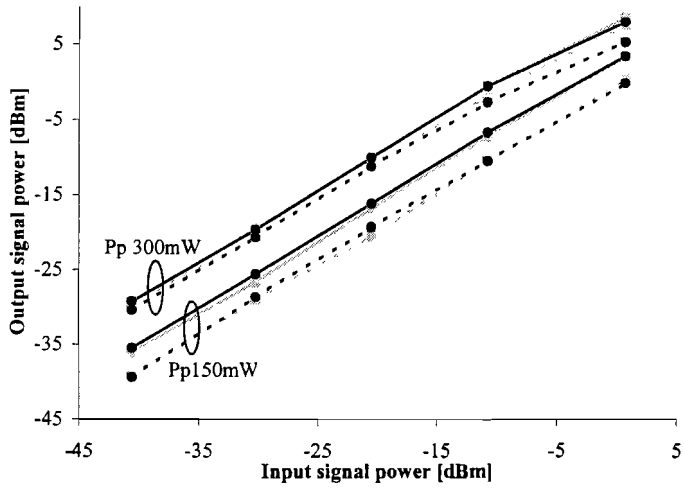

Figure 6.3.2 Output power versus input signal power for 150 mW and 300 mW of co- (●) and counter- (▒) propagating pump power. Signal wavelength is 1310 nm. Dashed lines represents 14 m and solid lines 7 m of fibre.

The signal power at the output is plotted versus the signal power at the input of the amplifier in figure 6.3.2. Almost no difference in shape exists between all of the output power curves. The short fibre length results in a slightly higher output power value. This is a result of the extra intrinsic fibre loss for the situation with two fibre modules. This difference decreases at higher pump powers. Probably, when applying more pump power, the loss will be more than compensated. This will lead then to higher gain and higher output powers.

If the slope of output power curve is 1, an increase in signal power will lead to the same increase of output power. A slope close to 1 will mean a near constant signal gain for a large signal power range. For 300 mW of pump power and 7 m of fibre these (average) slopes are 0.92 when co- and 0.93 when counter-directional pumped. For 14 m of fibre these values are respectively 0.88 and 0.92.

In figure 6.3.3 the fibre net gain is set out against the signal wavelength for a signal power of –20 dBm. The figure on the left side shows co- and the right figure shows counter-directional pumping. The gain profiles are almost similar shaped. For counter-propagating the gain is slightly higher. At higher pump power the longer fibre length results in higher net gain values.

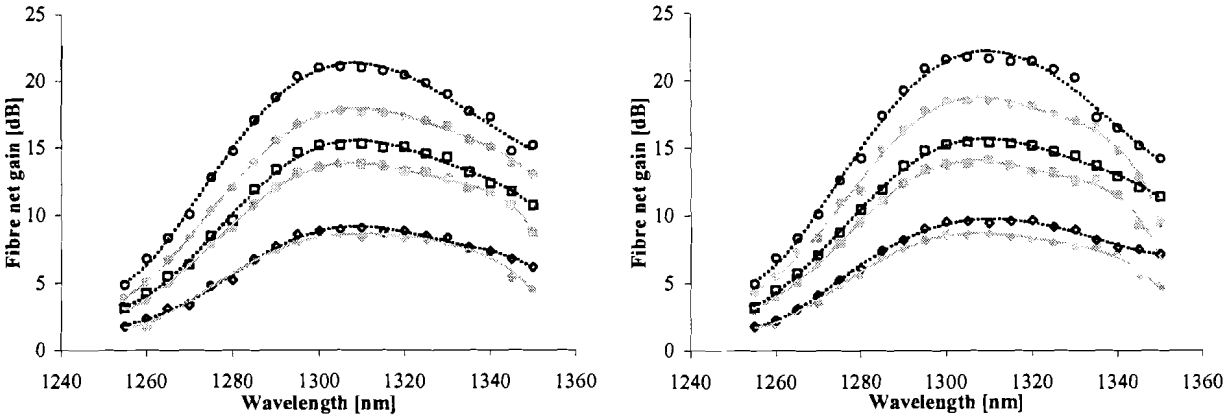

Figure 6.3.3 Fibre net gain versus wavelength for 100 mW (◆), 200 mW (■) and 300 mW (●) of pump power. Left side co-propagating, right side counter-propagating. Dashed lines represents 14 m and solid lines 7 m of fibre. Input signal power is –20 dBm.

The overall signal gains as shown in figure 6.3.4 are almost equal at the lower wavelengths in all situation, the pumping scheme does not alter signal gain. Above 1300 nm the short fibre length results in more gain. Some actual gain values are listed in appendix C.

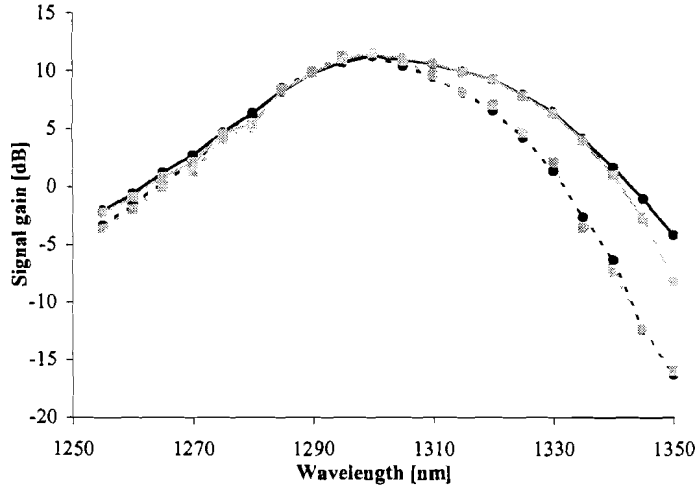

Figure 6.3.4 Signal gain with co- (●) and counter- (●) propagating pump powers of 300 mW. Dashed lines represents 14 m and solid lines 7 m of fibre. Input signal power is –20 dBm.

From the figure above some characteristically values are summarised in table 6.3. It can be seen from this table that the bandwidth turns out to be reduced for all amplifier configurations compared to small signal gain. For the short fibre the bandwidth is still larger and also co-pumping results in a little larger bandwidth. Maximum gain is still found at a wavelength of 1300 nm.

Table 6.3 Several amplifier characteristics for moderate signals (-20 dBm).

Pump scheme	*Fibre length* [m]	λ_{Gmax} [nm]	$Gain_{max}$ [dB]	λ_{min} [nm]	λ_{max} [nm]	B_{-3dB} [nm]
Co	14	1300	11.2	1288	1311	23
Counter	14	1300	11.5	1289	1310	21
Co	7	1300	11.2	1288	1320	32
Counter	7	1300	11.4	1289	1320	31

6.4 Large signal region

This region specifies signal powers around 0 dBm and above. Because of the restricted output power of the tunable laser source for signal generation the measurements are limited to a maximum signal power of around +1.5 dBm. In figure 6.4.1 the fibre net gain is plotted versus pump power using a signal of +1.4 dBm at 1310 nm for both co- and counter-directional pump with for 7 m or 14 m of fibre.

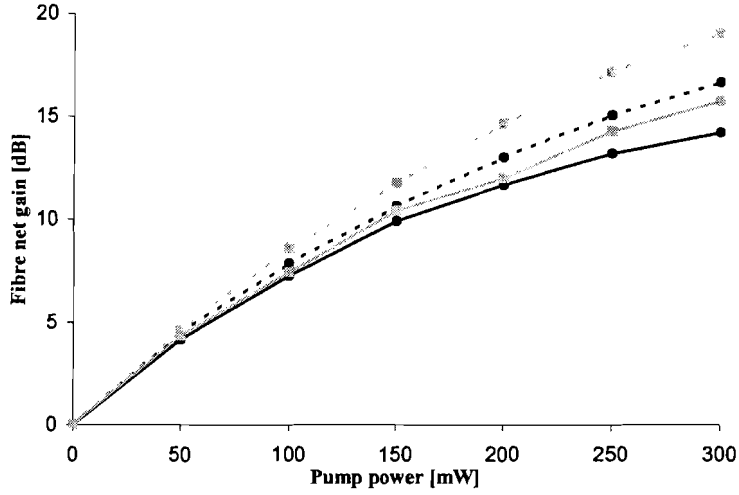

Figure 6.4.1 Fibre net gain versus pump power for a signal power of +1.4 dBm at 1310 nm. Co- (●) and counter- (●) propagating pump, dashed lines represents 14 m and solid lines 7 m of fibre.

At small pump powers the gain profiles do not differ much. But when increasing pump power, counter-propagating yields to a distinct higher gain. For 7 m of fibre the pump power efficiency is 0.073 dB/mW and 0.074 dB/mW for respectively a co- and counter-directional pump. For 14 m off fibre these values are respectively 0.079 dB/mW and 0.086 dB/mW. The extra fibre length pays of at higher pump powers. The relatively small difference in fibre net gain between 14 m co- and 7 m counter-pumping is noteworthy. It seems that for large signal powers, co-propagating pumping has

a stronger tendency to saturate. For counter-pumping there is no strong saturation effect present, especially for the long fibre length. It appears that for higher pumping power there is a potential higher gain possible.

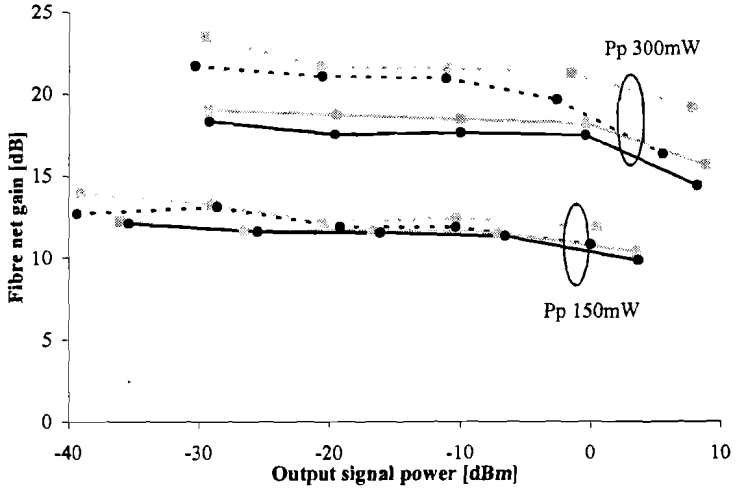

Figure 6.4.2 Fibre net gain versus output signal power for 150 mW and 300 mW of co- (●) and counter- (▒) propagating pump power. Dashed lines represents 14 m and solid lines 7 m of fibre. The signal wavelength is 1310 nm.

The fibre net gain is plotted versus output signal power in figure 6.4.2 for different pump powers. The differences observed in gain values are relatively small when 150 mW of pump power is being applied. The gain remains almost constant in the entire output power region. When applying more pump power the differences become more distinct. At higher output power, the extra fibre length results in higher signal gain. Again a constant gain is observed, but at high output powers there is a trend for the gain to saturate. This effect is strongest for a co-propagating pump scheme.

The point where the output power is saturated is of interest. This is the output power value where the gain has dropped –3 dBm. A saturated output power of +7.4 dBm is found for 7 m and +3.0 dBm for 14 m of fibre in the case of counter-propagating pumping with 300 mW of pump power. For the same situation only now co-propagating pumping, a saturated output power of around +5.7 dBm and –0.5 dBm is found for respectively 7 m and 14 m of fibre.

The overall signal gain spectrum, this is the signal gain without compensating for the fibre loss, is plotted for different amplifier configurations in figure 6.4.3.

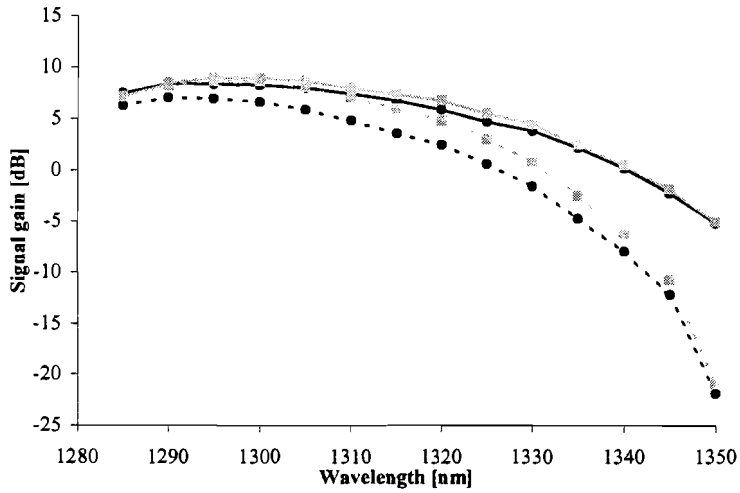

Figure 6.4.3 Signal gain (signal power is circa 0 dBm) with co- (●) and counter- (▩) propagating pump power of 300 mW, dashed lines represent 14 m and solid lines 7 m of fibre.

When the tunable laser source providing the input signal is set to a maximum output power, the signal power over the different wavelengths varies ±1 dB. In the wavelength region shown, the input signal power is approximately 0 dBm with an inaccuracy of ±1 dB. All gain profiles are at a reasonable even level, especially for the short fibre length. For 14 m of fibre the gain drops quickly when the wavelength is over 1330 nm. The short fibre length shows higher gain values. The highest signal gain is available when the amplifier is counter-pumped. According to table 6.4, maximum signal gain is achieved at a slightly lower wavelength compared to the other signal power regions. It is not possible to determine an accurate value for the amplifiers bandwidth caused by the variance in input signal power.

Table 6.4 Maximum amplifier signal gain for large signals (circa ±0 dBm).

Pump scheme	*Fibre length [m]*	λ_{Gmax} *[nm]*	$Gain_{max}$ *[dB]*
Co	14	1290	7.1
Counter	14	1295	8.7
Co	7	1295	8.4
Counter	7	1295	9.0

6.5 Discussion single-pass configuration

In appendix C the maximum achieved signal gain values are tabulated. This is done for the different amplifier pump schemes and signal regions.

Small signal region:

For small signal gain, co-propagating and counter-propagating pumps yield approximately the same gain and only the total amount of pump power matters. This is because the ASE patterns generated by the two pump schemes are mirror images of each other and so the average upper state population is the same in both cases. In the limiting case of a small signal, the signal is too weak at all points along the fibre, to influence or change the ASE patterns and hence the transfer of energy from pump to signal [1]. For small and moderate pump powers the difference in gain can be neglected and must be attributed to measurement inaccuracy.

A higher signal gain is measured for the counter-propagating pumping scheme at high pump powers. Perhaps when the amplifier is co-directional pumped, the fibre signal gain already inhibits some more saturation compared to counter-directional pumping. When counter-directional pumped the signal is strongest where the pump is strongest, allowing for an efficient transfer of energy between pump and signal without ASE absorbing too much of the pump energy. To put it in other words, the most advantageous situation is to have the signal strong where the inversion is strong, so that the signal, not the ASE, will deplete the gain. This especially applies for the case with two PDF modules, the ASE should start playing a role sooner with increased fibre length. Also the different loss in passive components for the two pump-schemes introduces some deviations in the comparison.

Moderate signal region:

As the signal power is raised, the choice of pumping direction between co- and counter-propagating pump starts to influence the signal gain of the amplifier. This is caused by the interaction between gain experienced by signal and that experienced by the forward- and backward-propagating ASE. In the case of inline amplifiers, with signal input levels in the –20 dBm to –10 dBm range, the counter-propagating pumping scheme performs better as the co-propagating one. This applies for sufficiently long fibres where ASE effects are playing a significant role. The counter-propagating pump yields a higher output power than the co-propagating pump at long fibre length, due to the pump level evolution along the fibre being better adapted to the signal growth. The signal power is strongest where the pump power is strongest. Thus allowing for an efficient transfer of energy

between pump and signal power without the ASE absorbing too much of the pump energy. The counter-propagating pump is also well suited in the case when pump ESA is present as the signal can more effectively deplete the inversion and reduce the pump ESA. At the shorter fibre lengths where the ASE is low and the fibre is well inverted the choice of pumping direction does not matter [1].
The measurement results show little difference in signal gain for short fibre length as well as low pump powers. At high pump powers and thus a large ASE contribution, the highest signal gain is obtained with the counter-propagating pump scheme, especially when the long fibre length is concerned.

Large signal region:
When the input signal power level increases the population inversion achieved by counter-propagating pumping is generally higher than with a co-propagating pump [2]. Higher population inversion means more available gain. This be the cause of a higher required pump power, in a saturated section in order to prevent any reduction in the population inversion due to the stimulated transition. For strong signals, 0 dBm and more, the choice of pumping direction does matter, in favour of the counter-directional pump scheme.

There is no noteworthy difference in signal gain when the applied pump power is small. At high pump power the counter-propagating scheme outperforms the co-propagating configuration. For the long fibre length the gain difference becomes even more in favour of the counter-directional pump scheme. Under these conditions the co-directional pumped fibre has strong signal gain saturation. The highest output power is available when counter-directional pumped.

6.6 Double-pass configuration

6.6.1 Introduction

Making the signal pass the fibre twice is an opportunity to benefit more of the amplification qualities of the doped-fibre. This is done by placing a Faraday rotator mirror (FRM) at the end of the fibre combined with an optical circulator at the input. The doped fibre is polarisation independent, so at first pass, the signal is amplified independent of polarisation state. The FRM reflects the signal with a 90 degrees shift in polarisation state. For the second pass all amplification is still available resulting in a more efficient use of the available fibre gain. This only applies when the amplifier remains far from the point where gain saturation occurs.

6.6.2 Double-pass measurements

The double-pass amplifier set-up used is depicted in figure 6.6.2.1. The input signal passes the optical circulator and the pump power is added in the WDM. These powers are then coupled into the doped fibre.

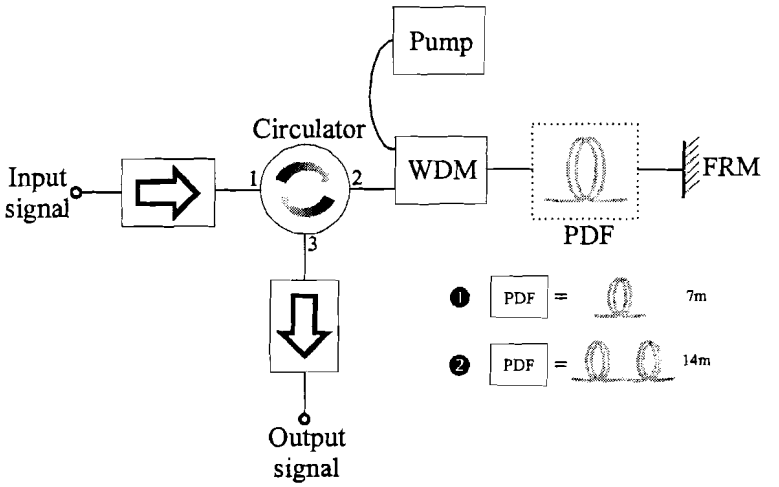

Figure 6.6.2.1 Double-pass amplifier measurement set-up. Configuration 1 consists out of 7 m of doped fibre. Configuration 2 has total active fibre length of 14 m.

At the end of the PDF module the signal is reflected by a FRM. The circulator directs the backward travelling signal to the output port. The signal isolators are unnecessary because the circulator also acts as isolator. Still they are used to make a more convenient comparison between single and double-pass set-up possible. Again the doped fibre length is 7 m or 14 m.

In figure 6.6.2.2 the net fibre gain is plotted versus signal wavelength for different signal powers. The highest signal gain is available for small signal powers. This becomes even more clearly at higher pump power values. At low pump powers the differences in signal gain between 7 m and 14 m of fibre are small. Appendix C lists some actual maximum gain values.

The extra available gain introduced by the increased length is compensated by the higher intrinsic fibre loss. At low pump powers the amplifier with short fibre length will result in higher output powers. For high pump powers the differences are more distinct. The long fibre length results in much higher net fibre gain values.

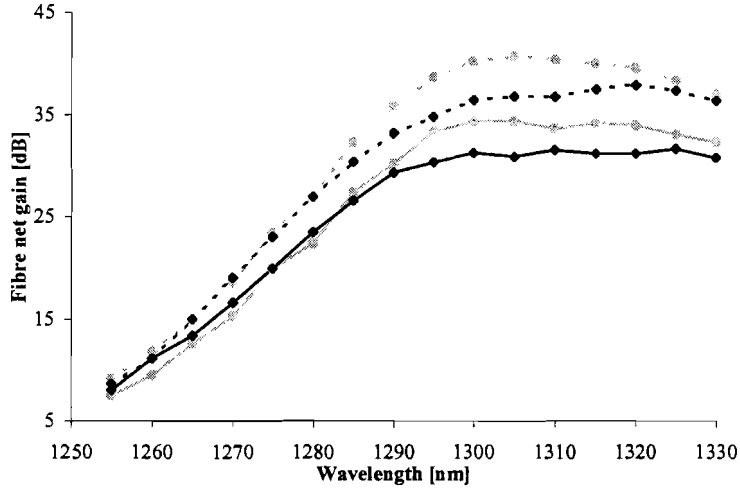

Figure 6.6.2.2 Fibre net gain versus wavelength for 300 mW of pump power. Signal power is –30 dBm (◈) and –10 dBm (◆). Dashed lines represents 14 m and solid lines 7 m of fibre.

It is also possible to determine the –3 dB bandwidth from the overall signal gain, this is not depicted in figure 6.6.2.2 but did serve as bases for the figure. This is done in table 6.6 for a small signal power of –30 dBm with 300 mW of pump power. An increase in fibre length strongly reduces the gain bandwidth of the amplifier, especially at higher wavelengths.

Table 6.6 Several small signal double-pass amplifier characteristics.

Fibre length [m]	λ_{max} [nm]	$Gain_{max}$ [dB]	λ_{min} [nm]	λ_{max} [nm]	B_{-3dB} [nm]
7	1300	20.7	1290	1316	26
14	1300	20.4	1289	1310	21

More pump power will probably increase the signal gain even more. This becomes clearer when looking at the fibre net gain in figure 6.6.2.3 where it is plotted versus pump power.

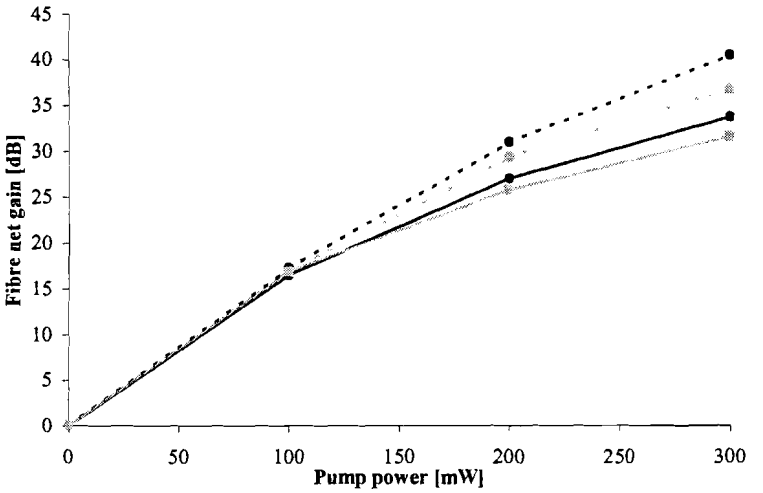

Figure 6.6.2.3 Fibre net gain versus pump power. Signal power is –30 dBm (●) and –10 dBm (▒) at 1310 nm, solid lines represent 7 m and dashed lines 14 m of fibre.

The slope of the gain curves all decline, but in a manner that increasing the pump power even further still results in higher signal gains. This is particularly the case for small signal gain. For 7 m of fibre the pump efficiency is 0.129 dB/mW for a signal power of –10 dBm and it is 0.135 dB/mW with a signal power of –30 dBm. For 14 m of fibre these values are 0.147 dB/mW respectively 0.155 dB/mW.

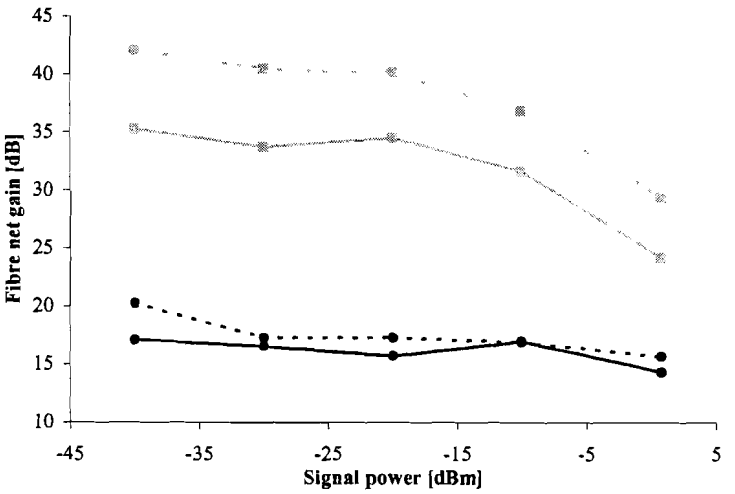

Figure 6.6.2.4 Fibre net gain versus signal power (1310nm) for 100 mW (●) and 300 mW (▒) of pump power. Dashed lines represent 14 m and solid lines 7 m of fibre.

Gain saturation caused by pump power will first manifest itself at the shortest fibre length. In figure 6.6.2.4 the fibre net gain is plotted versus the signal power for different pump powers. The highest gain is available in the small signal region. For small pump powers the fibre length is not an

important factor. The amplifier also shows no strong saturation for higher signal powers. At high pump power the signal gain differs in favour of the long fibre length. A considerably higher fibre net gain is achieved in all of the signal power range. Strong amplifier saturation is observed at large signal powers for both short and long fibre lengths.

The output signal power is plotted versus the input signal power on the left side of figure 6.6.2.5. The short fibre length results in the highest output powers caused by the lower fibre loss. But for high pump powers this difference decreases rapidly. Applying even more pump power could finally have as result that the highest output powers is achieved with the long fibre length.

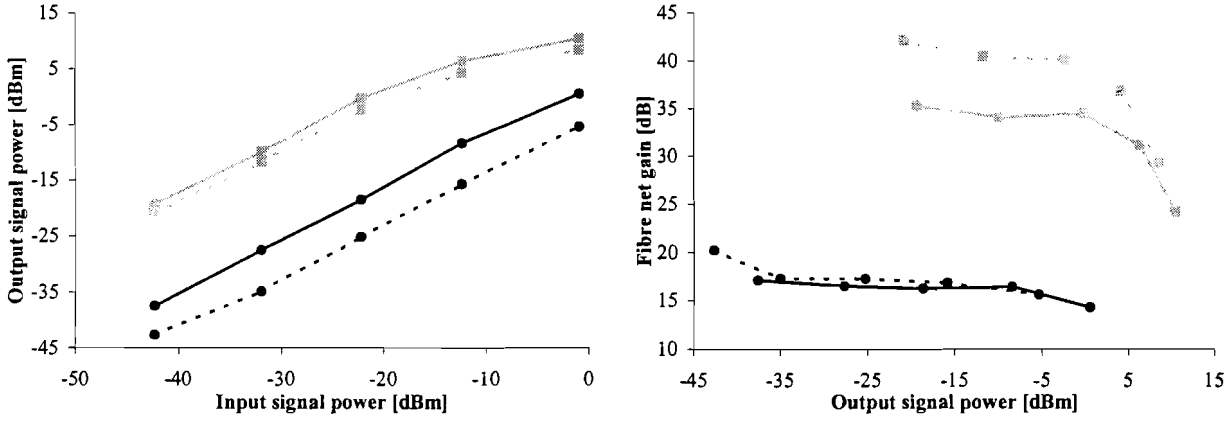

Figure 6.6.2.5 Left side: Signal output power versus signal input power at 1310 nm. For 100 mW (●) and 300 mW (▒) of pump power, dashed lines represent 14 m and solid lines 7 m of fibre. Right side: Fibre net gain versus signal output power under equal conditions.

The average slopes for 7 m of fibre are 0.93 with 100 mW of pump power and 0.74 for 300 mW of pump power. For 14 m of fibre the values are 0.92 respectively 0.73. An increase of input power leads to practically the same increase in output power for input signal below –15 dBm and 100 mW of pump power. Higher signal powers demonstrate slight amplifier gain saturation particularly at high pump powers.

The right side of the figure shows the fibre net gain versus output signal power for different values of pump power. For low pump power the signal gain remains almost constant for a large signal power span for both fibre lengths, this changes at high pump power. Strong gain saturation is observed stating at output powers of 0dBm, again for both fibre lengths. As mentioned before, the highest fibre net gain is reached for the long fibre length. The output power where the signal gain is

saturated (dropped –3 dB) is for 300 mW of pump power –1.4 dBm in the case of 14 m of fibre. For 7 m of fibre this saturated output power is +4.4 dBm.

6.6.3 Discussion double-pass configuration

First some general remarks. It is also possible to reflect the pump power at the fibre end. The doped fibre length is optimised for the amount of pump power available. Reflection of pump power would then be useless. In the double-pass configuration the fibre is pumped at the signal input. It is also possible to apply pump power at the other end of the fibre. From the discussion in 6.5 it follows that for small signals the way of pumping has little influence. But at higher signal powers the counter-propagating pump scheme is preferred if gain saturation is considered. The double-pass configuration is in a way comparable with first a co-propagating amplifier followed by counter-propagating amplifiers when power evolution along the fibre is considered. The small signal is applied to the co-directional pumped section and amplified. The larger signal is then applied to a counter-pumped amplifier. This is the preferred pumping direction when signal gain is considered. A double-pass configuration with a bi-directional pump scheme could as a result of the more uniform pump power distribution and higher population inversion lead to even higher small signal gain.
Reflections of the doped fibre ends have to be well below the fibre net gain. Otherwise the amplifier tends to work in the lasing regime. At least the noise performance suffers due to multi path interference (MPI) caused by these reflections [3].

The small signal bandwidth decreases with fibre length, to 26 nm for 7 m and 21 nm for 14 of active fibre. The single-pass amplifier has a small signal bandwidth of 37 nm when co-directional pumped. Double-passing the fibre strongly reduces gain bandwidth.

In the double-pass set-up high signal gain is available, especially in the small signal region. For 14 m of fibre the net gain almost compensates for the extra introduced fibre loss. Resulting in almost the same output powers as with 7 m of doped fibre. With even more pump power available the 14 m of fibre would lead to the highest small signal gain. The pump power efficiency for small signals has a maximum of circa 0.10 dB/mW for a counter-directional pumped single-pass set-up. This increases to circa 0.16 dB/mW for a double-pass set-up with 14 m of fibre. This emphasises the more efficient use of the fibres available signal gain in a double-pass configuration. At higher signal powers the active fibre gain saturates strongly. The average slope of output versus input power is approximately 0.7 for both fibre lengths at maximum pump power. For a single-pass set-up this

average slope is approximately 0.9 for both pumping schemes and fibre lengths. This indicates larger gain saturation by signal power in a double-pass set-up.

For a double-pass set-up with 7 m of fibre the saturated output power is +4.4 dBm and for 14 m this is –1.4 dBm. When co-directional pumped these values are +5.7 dBm and –0.5 dBm for 7 m respectively 14 m of fibre. For counter-directional pumping these values are +7.4 and +3.0 dBm. Indicating that a double-pass set-up has a much lower saturated output power especially when the single-pass amplifier is counter-directional pumped. It is easier to draw a comparison between the two single-pass and the double-pass amplifier configurations using the table of appendix C. The small signal gain is substantially higher when the signal passes the active fibre twice. For signal powers above –20 dBm the signal gain and the output powers start to saturate more in the double-pass configuration. Resulting in smaller gain differences and more comparable output powers. Contrasted to these other configurations the double-pass set-up is best used in the small signal region where the active fibre is less saturated.

6.7 Amplifier noise

6.7.1 Introduction

The excited praseodymium ion decays to its ground state either through stimulated emission caused by a signal photon or by spontaneously decay. A spontaneous emitted photon has random phase and direction. Some of these photons are captured by the propagating mode of the fibre and are amplified as they travel inside the doped fibre resulting in ASE. ASE is the main contributor in noise of an optical amplifier.
This noise will degrade the signal to noise ratio (SNR) at the receiver. The photo detector converts forward travelling ASE to beat noise. Subsequently increasing the bit error rate (BER) of an optical communication system.

6.7.2 Amplified spontaneous emission

The ASE spectra for the different pump schemes are examined. Figure 6.7.1 shows signal and ASE powers for a co- (left) and a counter- (right) propagating pump scheme. When no pump power is applied an ASE contribution is already present. The tunable laser source used to generate the signal is not shot-noise limited and also has a spontaneous emission contribution. The ASE observed at the PDFA output is composed of ASE from the laser source and from the amplifier itself.

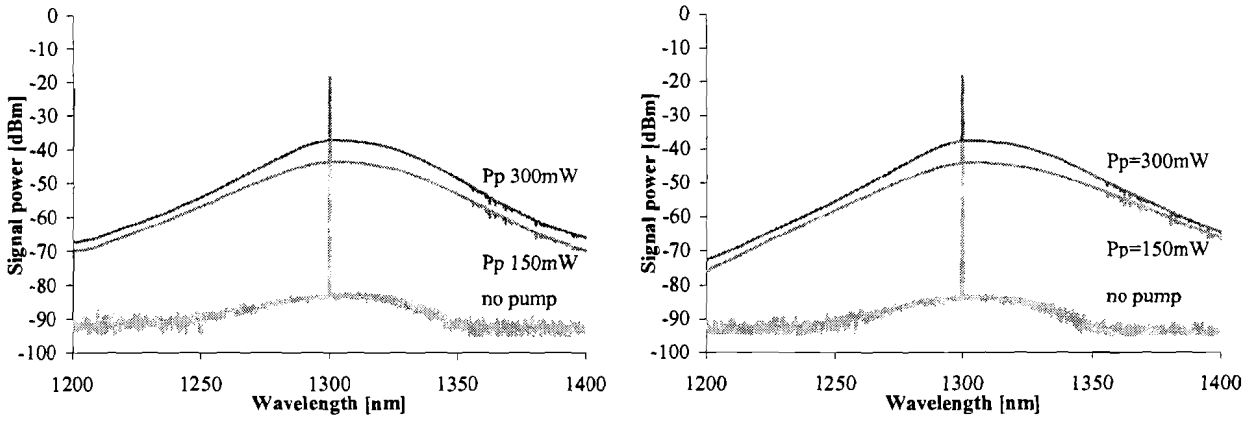

Figure 6.7.1 Typical output spectra for various pump powers with 7 m of fibre. Left side co- and right side counter-propagating pump. Signal power –30 dBm at 1300 nm.

Some small differences are observed between the pumping schemes. Co-propagating pump shows a higher ASE contribution at the lower wavelengths. The ASE contribution is almost similar for both pump schemes with a signal wavelength of 1300 nm. At higher wavelengths the ASE contribution is highest when counter-propagated pumped. When co-directional pumped the fibre is mostly inverted where the signal enters. The fibre losses are smallest for low wavelengths and over 1300 nm the loss rapidly increases. When counter-directional pumped the end of the fibre is mostly inverted. Losses at the higher wavelengths as a result of the GSA contribution will be minimised as the ground state is bleached from electrons.

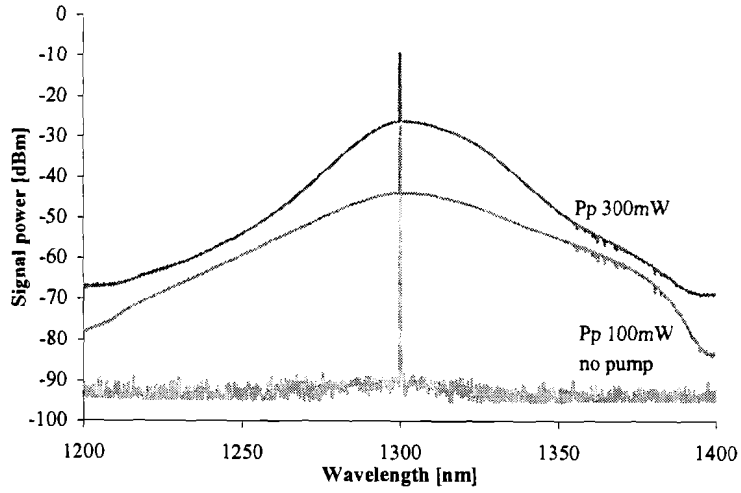

Figure 6.7.2 Output spectra at different pump powers for a double-pass set-up with 7 m of fibre. Signal power is –30 dBm at 1300 nm.

In figure 6.7.2 the output spectra are given of a signal double-pass configuration. Under these conditions it is hard to measure the noise generated by the amplifier when no pump power is applied. The high intrinsic losses cause the noise contribution of the amplifier to drop below the detection limit of the OSA. Only a part of the contribution of the spontaneous emission from the laser source is measured. With small amounts of pump power applied, the extra loss introduced by double-passing the fibre results in lower ASE values at the low and high wavelengths. The highest gain is available in a region around the signal wavelength. Powers double-passing in this region will highly benefit from the extra available gain and will more than compensate for the higher fibre losses. This therefore results in higher power values compared to a single-pass configuration. At even higher pump powers this gain region becomes more clearly perceptible.

6.7.3 Noise figure measurements

The measurements performed to determine the signal gain of the amplifier are performed with an OSA. Subsequently, the ASE contributions in the output spectrum are available. From this it is possible to determine the SNR at the output of the amplifier, simply by resolving the difference between signal top and noise level in close proximity of the signal wavelength. This is also done at the input side and from this the noise figure of the amplifier is calculated. The noise figure results derived from this method turn out to be impracticable.

When small signals are concerned the sensitivity of the OSA becomes a problem. When not pumped the amplifier output spectrum drops below the detection limit of the OSA. This is a result of the high losses of the amplifier set-up, especially when long fibre lengths or if a double-pass configuration is considered. Therefore the method is not suitable for small signals, especially when no pump power is applied.

The tunable laser source used to generate the input signals also has a contribution to spontaneous emission. This spontaneous emission is amplified and the measured output ASE is not only originating from the PDFA. Another problem is that the ASE must be found at the signal wavelength, so the ASE power must in some way be separated from the signal power.
It is desirable to distinguish amplifier noise behaviour related to the pump scheme used and to validate the simulation results with experimental results. The influences of connections and components used in the amplifier configuration have to be known exactly. Comparison between pumping scheme or a transformation to simulation conditions would otherwise not be possible.

6.7.4 Recommendations

In defining a measurement system to characterise PDFA noise figure, a number of problems must be solved. The ASE density must be measured at the signal wavelength, along with signal gain and photon energy. Normally a shot noise limited source is assumed. Most practical laser sources have spontaneous emission power present as well as the desired signal itself. The effect of source spontaneous emission (SSE) on the noise figure measurement must be found. Measurement of the ASE power density requires knowledge of the noise bandwidth of the optical spectrum analyser. The relationship between the displayed OSA resolution bandwidth and the effective noise bandwidth must be considered, as well as any wavelength dependence of this parameter. Since the ASE must be found at the signal wavelength, techniques are required either to estimate the ASE density, or to reject the signal to allow the ASE measurement at the signal wavelength.

An optical filter should be added to reduce SSE. The best way to vary the source laser power is with an optical attenuator. With an optical attenuator following a laser source operating at high output power, every dB of attenuation corresponds to the same reduction in input SSE noise power. To measure an amplifier noise figure, some more advanced an accurate methods are advised. The following measurement technique are extracted from [4] and [5].

Interpolation method:

This is a simple technique and allows for rapid measurement throughput. Since the signal occupies the same wavelength at which the ASE power must be measured, interpolation must be used to estimate the ASE noise power. Measurements of the noise power are performed adjacent to the amplified source signal. The ASE power is found by straight-line interpolation.
One method to correct for the SSE is to measure it without the PDFA in place, multiply it by the measured PDFA gain at that wavelength and subtract the result from the measured ASE power density with the PDFA in place.

Polarisation extinction method:

This method uses a polarisation state controller at the output of the PDFA followed by a polarizer that is connected to an OSA. The polarisation controller must be able to transform the incident polarisation state to a linear state that can be passed or rejected by the polarizer. The SSE is polarised and the polarisation controller can be set such that the source signal and spontaneous emission are rejected by the polarizer and prevented from reaching the OSA. The ASE power

density measured in one half the total PDFA ASE power when equal power in both polarisation modes is assumed [6].

Pulse-recovery method:

The pulse-recovery technique can make ASE measurements at the actual signal wavelength. The source is gated on and off with an optical switch with a fast fall time. The gated-on time needs to be long enough so that the PDFA stabilises to its steady state for the input signal [7]. Once the PDFA is in its steady state, the switch rapidly extinguishes the signal incident on the PDFA. Immediately after the signal is gated off, the ASE level at the amplifier output will be comparable to the true PDFA ASE without any SSE.

6.8 Conclusions

First the single-pass configuration is considered. The long fibre length resulted in the highest net fibre gain. But as a consequence of the higher intrinsic loss this results in lower output powers compared to the short fibre. These losses are especially noticeable at higher wavelength, and compress the gain bandwidth. The long fibre length only becomes an option when higher pump powers become available. This can more than compensate for the losses and result in higher signal gain and higher output powers, especially in the small signal region where the amplifier remains far from gain saturation.

In this region the pumping direction is of no influence on signal gain. At moderate signal powers the pumping direction does not matter for short fibre. But for 14 m of fibre, the counter-propagating pump results in higher signal gain compared to co-pumping. At even higher signal powers, 0 dBm or more the co-directional pumped amplifier is preferred for both lengths. Resulting in higher signal gain and output powers, whereas the co-directional pumped amplifier is more gain saturated.

When considering fibre length in a double-pass set-up, the same applies for the single-pass configuration; the extra available gain only compensates for the increased fibre loss and does not result in higher output powers. Also the gain bandwidth is compressed for 14 m of fibre length but the bandwidth is also reduced more due to passing the fibre twice. The only way to benefit from the enlarged fibre is to couple more pump power into the fibre. A bi-directional pump scheme could be a way to realise this.

The signal gain benefits most from a double-pass set-up in the small signal region. Much higher signal gains are achieved compared to a single-pass amplifier. At higher signal powers the double-pass set-up still results in higher signal gain and output powers, but strong gain saturation is present.

For large signals the advantage of a double-pass set-up is reduced, the amplifier is best used in the small signal region.

With the used measurement method it is not applicable to determine the amplifier noise figure in a satisfying manner. More advanced techniques are necessary for accurate noise figure measurements. Knowledge of the exact loss of every component used in the amplifier set-up is essential to valid simulation results and to distinct pump scheme influences on the noise figure.

7 Conclusions and recommendations

7.1 Conclusions

Concluded from chapter 4 is that the model results in general satisfy experimental results. For the lower signal wavelengths the model is less suitable, a better-determined background loss value can improve the match between simulation and experiment in this region. This less suitable region partly increases to higher wavelengths at increasing fibre length. The model remains valid around the important 1300 nm wavelength region. The mismatch between simulated and experimental results is mainly caused by fibre parameter deviations and by aberrations caused by the measurement system and method.
The measurement system makes it difficult to translate experimental to simulated conditions accurately. The inaccuracies introduced by the measurement method also complicate model validation.

Gain saturation is measured earlier and heavier by high signal and pump powers compared to simulation results of the active fibre. In the model effects like pump- and signal-ESA and co-operative upconversion are neglected. Also the non-radiative transitions, which shorten emission lifetime, are ignored. These effects are all gain-limiting resulting in earlier gain saturation of the amplifier.
Input signal powers of –40 dBm launched into the active fibre are around the limit for results without calculation errors when moderate fibre lengths are concerned. These signal powers will, at long fibre lengths, result in substantial numerical errors already at the higher wavelengths.

From the experimental results it is concluded that for single- and double-pass configuration, the long fibre length resulted in the highest net fibre gain, but as a consequence of the higher intrinsic loss this results in lower output powers compared to the short fibre. The loss is especially noticeable at higher wavelength and compresses the gain bandwidth. The ASE contribution also increases with fibre length. The long fibre length only becomes an option when higher pump powers become available, which would then more than compensate for the losses and result in higher signal gain and higher output powers. This especially applies in the small signal region where the amplifier remains far from gain saturation.

For a single-pass configuration the pumping scheme has a minor effect on the signal gain when small and moderate signal powers are concerned. The counter-directional pump scheme yields slightly higher gain, while the co-directional pumped scheme will improve the amplifier noise behaviour, especially when a relatively long active fibre is used. The passive components used alter the amplifier noise behaviour and possibly compensate for the improvement achieved by the pumping scheme. The counter-propagating pump scheme clearly outperforms the co-propagating pump scheme when large signals are concerned, displaying more signal gain and higher output power values. This is mainly caused by signal gain saturation, especially when co-directionally pumped.
The fibre amplifying properties are used more efficiently when the signal passes the fibre twice, resulting in higher output power values. The signal gain benefits most from a double-pass set-up in the small signal region. Much higher signal gains are achieved compared to a single-pass amplifier. At higher signal powers the double-pass set-up results in higher signal gain and output powers, but strong gain saturation is present, reducing the advantage of a double-pass set-up. So the double-pass amplifier is best used in the small signal region.

The current measurement method is not suitable to determine the amplifier noise figure in a satisfying manner. More advanced techniques are necessary for accurate noise figure measurements. Furthermore, knowledge of the exact loss of every component used in the amplifier set-up is essential to validate simulation results and to determine pump scheme influences on the noise figure.

7.2 Recommendations

The diversity of connectors and fibre types used in the amplifier set-up is a problem. The praseodymium-doped fibre modules have straight (FC-PC) connectors where the WDM uses angled (FC-APC) connector types. Thus hybrid patch cords are needed to connect both. All leading to coupling losses and limiting the pump power coupled in the active fibre. When replacing the connectors with splices this will benefit in higher effective gain, better noise performance and the possibility of coupling more pump power into the praseodymium fibre. More pump power will lead to higher signal gain and output powers. Also the change of system failure, due to breakdown of a connector, at high power connections is reduced. Of course this will drastically reduce the flexibility in experimental set-ups and in possible amplifier configurations.

Only simulated results with a bi-directional pumping scheme are discussed, because of the availability of only one WDM. In all experiments a double-output, ytterbium fibre laser is used as pump source. For co- and counter-directional pumping only one output is used. When using isolators with low insertion loss in the pump path (to protect the pump laser from residual pump power), the total pump power coupled into the fibre can be increased. The possibility of applying much higher pump powers in a bi-directional pumping scheme leads to superior gain performance, especially when combined with a double-pass set-up.
Other possible interesting amplifier configurations with two WDMs are for instance a cascade of two amplifiers, leading to a two-stage co-propagating or counter-propagating amplifier. When using a bi-directional set-up with two fibre modules, it is possible to separate the modules with an isolator. Thus creating a two-stage amplifier built up with a co-propagating amplifier cascaded with a counter-propagating amplifier. The isolator reduces the backward ASE coupled into the first amplifier section.

All experiments are performed with CW-signals; a next step would be performing some dynamic experiments, for instance gain measurements and amplifier distortion- and noise-measurements using modulated input signals. Also the distortion of this signal by using a double-pass in comparison with a single-pass set-up is an issue. Several amplifier applications on a systems level are of interest: BER-measurements in a data transmission link incorporating a PDFA, investigation of amplifier behaviour in a WDM transmission system. Another possibility is to integrate a PDFA in some kind of re-circulating loop, simulating large transmission distances, or simulating a multiplicity of consecutively placed PDFAs.
When a bi-directional amplifier becomes operable it will be possible to validate the bi-directional pumped simulation results in chapter 5. The validation of the noise figure simulation results with one of the recommended measurement methods is also of importance. Improved experimental conditions, for instance reducing the connections, and more accurate knowledge of component losses will enable a better translation between experimental and measurement conditions.

The same applies for the model input data. A more accurate determined background loss, coupling loss and experimental determined ESA cross-section will all contribute to better matching conditions.
For some applications, an enhancement of the model is required. To get an insight in population densities at the different levels or of the population inversion in the metastable level, some kind of

simulation would be convenient. This requires a whole different set-up of the used solving method. This is also the case when simulating a double-pass set-up becomes an issue.
All simulations are solved for steady-state conditions. This satisfies for validating CW-experiments. When dynamic amplifier behaviour becomes an issue this will no longer be sufficient. Some kind of temporal behaviour model would be necessary, making simulations on signal distortions in the time domain possible.
Simulating more on systems point of view could be convenient, perhaps considering effects of cascaded amplifiers in a communication link, making judgements on preferred modulation scheme or maximum bit rate possible. Also noise problems and time-critical problems become of interest.

References

References chapter 1

[1] R.J. Mears, L. Reekie, I.M. Jauncey, D.N. Payne
"Low-noise erbium-doped fibre amplifier operating at 1.54 μm"
Electronics Letters, vol. 23, p1026 (1987)
[2] Y. Ohishi, T. Kanamori, T. Kitagawa, S. takahashi, E. Snitzer, G.H. Sigel, Jr.
Optics Letters, vol. 27, p1747 (1991)
[3] S.F. Carter, D. Szebesta, S.T. Davey, R. Wyatt, M.C. Brierly, P.W. France
Electronics Letters, vol. 27, p628 (1991)
[4] Y. Durteste, M. Monerie, J. Y. Allain, H. Poigant,
Electronics Letters, vol. 27, p626 (1991)
[5] K. Wei, D.P. Machewirth et al.
Journal of Non-Crystal Solids, vol. 182, p257 (1995)
[6] M.C. Brierly, S. carter, P.W. France, J. Peterson
Electronic Letters, vol. 26, p329 (1990
[7] P.C. Becker, N.A. Olsson, J.R. Simpson
"Erbium-doped fiber amplifiers: fundamentals and technology"
Academic press (1999)
[8] J. Heo, Y.B. Shin, H.S. Kim
"Dy^{3+}-doped GeGaSKBr glasses for the 1.3 μm fiber amplifier materials"
WG7-1993
[9] B.N. Samson, J.A. Medeiros Neto, R.I. Laming, D.W. Hewak
"Dysprosium doped GaLaS glass for an efficient optical fibre amplifier operating at 1.3 μm"
Electronics Letters, vol. 30, p1617 (1994)
[10] L.B. Shaw, B.J. Cole, J.S. Sanghera, I.D. Aggarwal, D.T. Schaafsma
"Dy-doped selenide glass for 1.3 μm optical fiber amplifiers"
OFC'98 Technical Digest, p141 (1998)
[11] L.F. Tiemeijer
"High performance MQW laser amplifiers for transmission systems operating in the 1310 nm window at bitrates of 10 Gb/s and beyond"
Proc. 21st Eur. Conf. on Opt. Comm. ECOC'95 (1995)
[12] D. Sigogne, A. Ougazzaden, B. Mersali, J. Landreau, C. Amra, A. Ranane
"1.55 μm polarization insensitive InGaAsP strained MQW optical amplifier with a high confinement factor"
Proc. 21st Eur. Conf. on Opt. Comm. ECOC'95 (1995)
[13] S.V. Chernikov, Y. Zu, R. Kashyap, J.R. Taylor
"High-gain, monolithic, cascaded fibre Raman amplifier operating at 1.3microns"
Electronic letters, vol.31, p472 (1995)
[14] S. Namiki, Y. Emori
"Recent advances in ultra-wide Raman amplifiers"
Proc. of Optical Fiber Conference 1999

References chapter 2

[1] Y.K. Park, J.M.P. delavaux, O. Mizuhara, L.D. Tzeng, T.V. Nguyen, M.L. Kao, P.D. Yeastes, S.W. Granlund, J. Stone
"Ninety-two photons/bit sensitivity using an optically preamplified direct-detection receiver"
Conf. on Opt. Fiber Comm., OSA Technical digests series, vol. 5, p.245 (1992)
[2] Y.K. Park, S.W. Granlund
Optical Fiber Technology, vol. 1, p59 (1994)
[3] Becker, P.C., Olsson, N.A., Simpson, J.R.
"Erbium-doped fibre amplifiers: Fundamentals and technology"
Academic Press, London (1999)
[4] R.W. Hellwarth
Physics Review, no. 130, p1850 (1963)
[5] A.R. Chraplyvy
Electronic Letters, vol. 20, p58 (1984)
[6] M. Yamada, M. Shimizu, Y. Ohishi, J. Temmyo, T. Kanamori, S. Sudo
"High efficient configuration of a Pr^{3+}-doped fluoride fiber amplifier module with an optical circulator"
Photonics Technology Letters, vol. 5, no. 9, p1011-1013 (1993)
[7] S. Wannenmacher
"Praseodymium doped fibre amplifier for optical amplification at 1300nm
Globecom conference 1996
[8] V. Morin, E. Taufflieb
"High output-power praseodymium-doped fiber amplifier single-pumped at 1030 nm: analysis and results
IEEE Journal of Quantum Electronics, vol. 3, no. 4, p1112 (1997)

References chapter 3

[1] S.T. Davey, P.W. France
BT Technology journal, vol. 7, p58 (1989)
[2] Ohishi, Y., Kanamori, T.,Nishi, T., Takahashi, S., Snitzer, E.
"Concentration effects on gain of Pr^{3+}-doped fluoride fibre for 1.3 μm amplification"
IEEE Photonics Technology Letters, vol. 4, p1338-1341 (1992)
[3] Y. Ohishi, T. Kanamori, T. Nishi, S. Takahashi
"A high gain, high output saturation power Pr^{3+}-doped fluoride fibre amplifier operating at 1.3 μm"
IEEE Photonics Technology Letters, vol. 3, p715-717 (1991)
[4] Y. Ohishi, T. Kanamori, T. Nishi, S. Takahashi, E. Snitzer
"Concentration effect on gain of Pr^{3+}-doped fluoride fibre for 1.3 μm amplification"
IEEE Photonics Technology Letters, vol. 4, no. 12 (1992)
[5] A. Remilleux, B. Jacquier, C. Linarès, C. Lesergent, S. Artigaud, D. Bayard, L. Hamon, J.L. Beylat
"Upconversion mechanisms of a praseodymium-doped fluoride fibre amplifier"
Journal of Physics D: Applied Physics, vol. 29, p963-974 (19960
[6] A.W.H. van Osch
"Modelling of praseodymium-doped fluoride fibre and sulfide fibre amplifiers for the 1.3 um wavelength region"
EUT report 95-E-294 (1995)

[7] M. Karasek
"Numerical analysis of Pr^{3+}-doped fluoride fibre amplifier"
IEEE Photonics Technology Letters, vol. 4, no. 11 (1992)
[8] Artiglia, M., P. di Vita, M. Potenza
"Optical fibre amplifiers: Physical model and design issues"
Optical Quantum Electronics, vol. 26, p585-608 (1994)
[9] Giles, C.R., E. Desurvire
"Modelling Erbium-doped fibre amplifiers"
Journal of Lightwave Technology, vol. 9, no. 2, p271-283 (1991)
[10] Jeunhomme, L.B.,
"Single-mode fibre optics: Principles and applications"
New York: Marcel Dekker, 1983
[11] Olsson, N.A.
"Lightwave systems with optical amplifiers"
Journal of Lightwave Technology, vol. 7, no. 7, p1071 (1989)
[12] Nabuurs, F.G.
"The TUE PDFA: Modelling of the noise figure and prediction of the gain and noise figure"
Student practical work report, TUE TTE-ECO, January 1997

References chapter 5

[1] Digonnet, M.J.F.
"Closed-form expressions for gain in three- and four-level laser fibers"
IEEE Journal of Quantum Electronics, vol. 26, no. 10, p1788-1796 (1990)
[2] Ohishi, Y., Kanamori T., Nishi, T., Takahashi, S., Snitzer, E.
"Concentration effects on gain of Pr^{3+}-doped fluoride fibre for 1.3 μm amplification"
IEEE Photonics Technology Letters, vol. 4, no. 12 p1338-1341 (1992)
[3] Ohishi, Y., Kanamori T., Nishi, T., Takahashi, S.
"A high gain, high output saturation power Pr^{3+}-doped fluoride fiber amplifier operating at 1.3 μm"
IEEE Photonics Technology Letters, vol. 3, p715-717 (1991)
[4] Nishida, Y., Yamada, M., Kanamori, T., Kobayashi, K., Temmyo, J., Sudo, S., Ohishi, Y.
"Development of an efficient praseodymium-doped fiber amplifier"
IEEE Journal of Quantum Electronics, vol. 34, no.8, p1332-1339 (1998)
[5] Artiglia, M., di Vita, P., Potenza, M.
"Optical fibre amplifiers: Physical model and design issues"
Optical Quantum Electronics, vol. 26, p585-608 (1994)
[6] Quimby, R.S., Zheng, B.
"Excited state absorption in Pr3+-doped fluorzirconate glass"
Applied Physics Letters, march 1992
[7] A.W.H. van Osch
"Modelling of praseodymium-doped fluoride fibre and sulfide fibre amplifiers for the 1.3 μm wavelength region"
EUT report 95-E-294 (1995)
[8] Ohishi, Y., Yamada, M., Kanamori, T., Terunuma, Y., Sudo, S.
"Analysis of gain characteristics of bi-directionally pumped praseodymium-doped fibre amplifiers"
IEEE Photonics Technology Letters, vol. 8, no.4, p521-514 (1996)
[9] Armitage, J.R.
"Three-level fiber laser amplifier: A theoretical model"
Applied Optics, vol. 27, no. 23, p4831-4836 (1988)

[10] Ohishi, Y., Yamada, M., Kanamori, T., Terunuma, Y., Shimizu, M., Sudo, S.
"Investigation of efficient pump scheme for Pr^{3+}-doped fluoride fiber amplifiers"
IEEE Photonics Technology Letters, vol. 6, no.2, p195-198 (1994)
[11] Becker, P.C., Olsson, N.A., Simpson, J.R.
"Erbium-doped fibre amplifiers: Fundamentals and technology"
Academic Press, London (1999)
[12] Baney, D., Hentschel, C., Dupre, J.,
"Optical fiber amplifiers: Measurement of gain and noise figure"
Hewlett-Packard Lightwave symposium 1993

References chapter 6

[1] Becker, P.C., Olsson, N.A., Simpson, J.R.
"Erbium-doped fibre amplifiers: Fundamentals and technology"
Academic Press, London (1999)
[2] Ohishi, Y., Yamada, M., Kanamori, T., Terunuma, Y., Sudo, S.
"Analysis of gain characteristics of bi-directionally pumped praseodymium-doped fibre amplifiers"
IEEE Photonics Technology Letters, vol. 8, no.4, p521-514 (1996)
[3] Gimlett, J.L., Cheung, N.K.
"Effects of phase-to-intensity noise conversion by multiple reflections on gigabit-per-second DFB laser transmission systems"
Journal of Lightwave Technology, vol. 7, no. 6, p888-985 (1989)
[4] Derickson, D.
'Fiber optic test and measurement"
Hewlett-Packard Books, Prentice Hall 1998
[5] Baney, D., Hentschel, C., Dupre, J.,
"Optical fiber amplifiers: Measurement of gain and noise figure"
Hewlett-Packard Lightwave symposium 1993
[6] Aspell, J., Federici, J.F., Nyman, B.M., Wilson, D.L.
"Accurate noise figure measurements of erbium-doped fiber amplifiers in saturation conditions"
Conf. On Opt. Fiber Comm., Opt. Society of America, paper ThA4 (1992)
[7] Baney, D.M., Dupre, J.
"Pulsed-source technique for optical amplifier noise figure measurement"
Eur. Conf. on Opt. Comm. ECOC'92, paper WeP2.11, p509-512 (1992)

Appendix A: Praseodymium-doped fluoride fibre module

Specifications:

Outer Dimensions 120 × 120 × 8.5 mm

Praseodymium doped Fibre (Fluoride Fiber)

Glass Composition	InF_3-based fluoride glass
Praseodymium concentration	1000 ppm
Fiber Structure	Core Diameter = 1.8 - 2.0μm Cut-off wavelength: 0.95 μm, Δn=2.5%
Length	7 m
Scattering Loss	<0.1 dB/m (for Δ n=2.5% fibers)
Background loss	<0.1 dB/m for 7 m of fiber

Pigtail Fiber(Silica Fiber)

Fiber Structure	Cut-off wavelength: 0.95 μm, Δn=0.45%
Connector type	FC-PC

Splicing

Splicing Loss	<0.5 dB/point
Return Loss	>50 dB/point (for Δn=2.5%fibers)

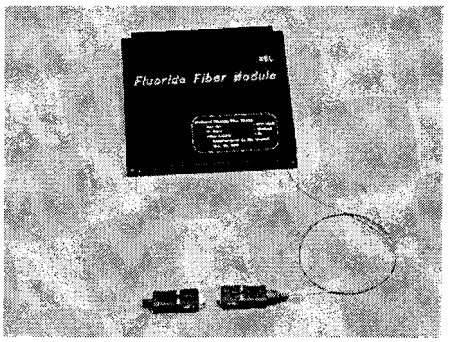

Appendix B: Automated measurement set-up

The measurement set-up is automated because of the high quantity of measurements that had to be performed on the PDFA set-up, in all the different possible configurations.

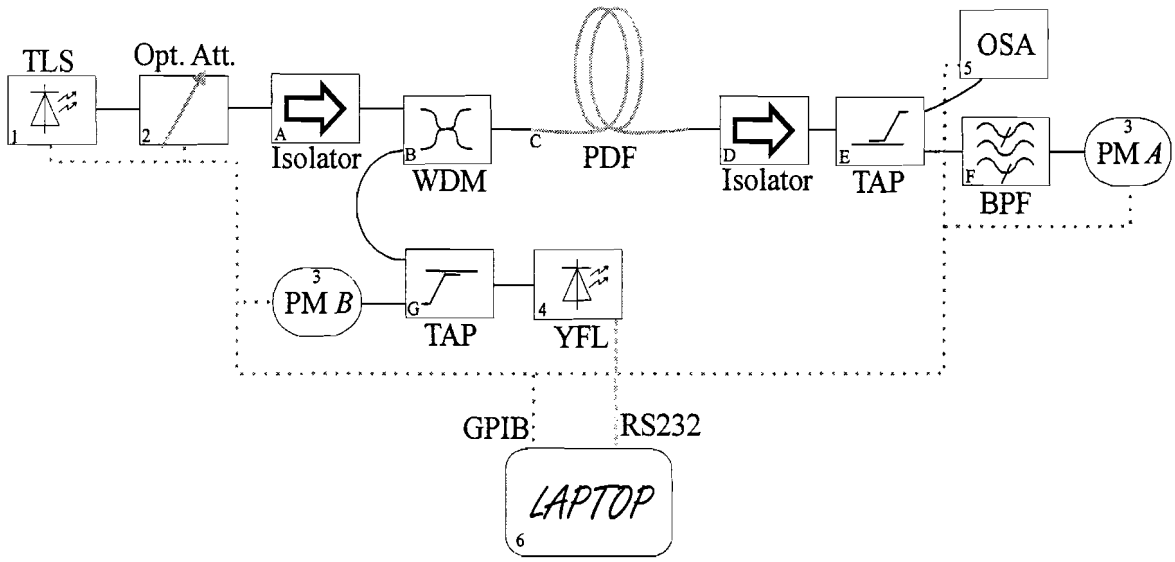

Figure B Example of a co-directional pumped fibre amplifier in an automated measurement set-up.

Listed below are the measurement instruments that are used in the set-up:

1 HP8167B 1300nm Tunable Laser Source
2 HP8156A Optical Attenuator
3 Newport 2832C Dual-channel Power meter
4 Ytterbium Fiber Laser 1030 nm 2 x 500 mW optical output
5 HP86145A Optical Spectrum Analyzer
6 Laptop with serial communication port and GPIB card

The different components used in the amplifier configuration are listed in the table B.

Table B Components used in measurement set-up.

	Component	*Manufacturer*	*Part number*	*Remarks*
A	Isolator	Isowave	X0388	1300 nm
B	WDM	IPFO	V362	1030/1310 nm
C	PDF module	NEL	9004/9005	7 m fibre/module
D	Isolator	TECOS	TIDA U3036	1300 nm
E	Tap coupler	Krone	97-328	1300 nm 50-50%
F	Band pass filter	TECOS	EC388L	1 nm / 1300 nm
G	Tap coupler	IPFO	V363	1030 nm 1-99%

All devices are controlled by laptop using GPIB for communication except for the YFL driver that uses RS232 for communication. For all devices several individual Labview drivers are written, Labview is a visual programming environment. The drivers are then combined and adapted for the different measurements. Some possible measurements are:

Signal wavelength sweep: with the power meter or optical spectrum analyser (OSA) the input or output power is measured as the signal wavelength sweeps through a defined range with a controllable wavelength interval.
Pump power sweep: with the power meter or OSA the input or output power is measured as the pump power sweeps through a defined range with a controllable interval of the pump power. The second channel of the power meter is connected to a 2% tap or WDM output for use as pump power monitor.
Signal power sweep: with the power meter or OSA the input or output power is measured as the signal power sweeps through a defined range with a controllable interval of the signal power. The tunable laser is set to the highest output power possible and then attenuated by the optical attenuator to acquire the desirable signal power. This is done to obtain the highest SNR possible at the input of the PDFA. All the measurements mentioned above can be combined in any required way. For example a signal power sweep combined with a pump power sweep, to get an output power spectrum at different pump powers.

A signal power sweep combined with a pump power sweep, incorporating a narrow band filter at the output to perform gain measurements or to perform saturation measurements. A handicap is that a filter is required to perform gain measurements with a power meter because of the power density of the ASE. This filter is normally hand-tuned so it can only be used at a constant signal wavelength. Using an OSA to perform the gain measurements circumcises the use of a filter and the restriction of a constant signal wavelength. Just by subtracting the input spectrum from the output spectrum the gain is obtained. But the spectrum also contains information of the signal to noise ratio and ASE at the output so it is possible to get hold of the noise figure of the amplifier. To do these measurements all input signals had to be defined. So first the signal spectra coming from the tunable laser source combined with the optical attenuator had to be measured. This is done for different wavelengths (range 1255-1350 nm) and powers (-40 to +4 dBm). The output spectra were measured with the defined input power spectra, this was possible due to the stability and reproducibility of the tunable laser source combined with the optical attenuator.

Appendix C: Maximum signal power and gain values

In the table below the maximum measured signal gain values are listed. This is done for all different amplifier configurations. All measurements are performed with 300 mW of pump power. First listed are the different amplifier configurations. Next the wavelength were maximum net fibre gain is achieved (λ_{max}). This gain ($G_{net\ fibre,max}$) is not the actual gain but the difference between pumped and unpumped fibre gain. The last 4 columns list the wavelength, the input and output power and the maximum overall gain (G_{max}). This gain is measured from isolator to isolator.

Table C: Maximum measured signal gain and powers for different amplifier configurations.

Configuration	λ_{max} [nm]	$G_{net\ fibre,max}$ [dB]	λ_{max} [nm]	$P_{signal,in}$ [dBm]	$P_{signal,out}$ [dBm]	G_{max} [dB]
Co-Propagating 7 m	1305	18.7	1300	-40.6	-28.5	12.1
	1305	17.8	1300	-30.1	-18.7	11.4
	1305	17.8	1300	-20.5	-9.3	11.2
	1310	17.5	1300	-10.6	+0.4	11.0
	1295	14.6	1295	0.0	+8.4	8.4
Co-Propagating 14 m	1305	21.9	1300	-40.6	-28.8	11.8
	1305	21.3	1300	-30.1	-18.9	11.2
	1305	21.1	1300	-20.5	-9.3	11.2
	1305	20.2	1295	-10.6	-0.3	10.3
	1300	16.8	1290	-0.5	+6.6	7.1
Counter-Propagating 7 m	1300	19.2	1300	-40.6	-28.5	12.1
	1310	18.8	1300	-30.1	-18.6	11.5
	1310	18.5	1300	-20.5	-9.1	11.4
	1305	18.2	1300	-10.6	+0.5	11.1
	1300	15.8	1295	0.0	+9.0	9.0
Counter-Propagating 14 m	1315	24.0	1300	-40.6	-28.1	12.5
	1305	21.7	1300	-30.1	-18.7	11.4
	1305	21.8	1300	-20.5	-9.0	11.5
	1305	21.3	1300	-10.6	+0.3	11.0
	1310	19.2	1295	0.0	+8.7	8.7
Double-pass 7 m	1305	35.3	1300	-40.6	-18.9	21.7
	1305	34.4	1300	-30.1	-9.4	20.7
	1310	34.5	1300	-20.5	-0.5	20.0
	1320	31.7	1300	-10.6	+6.4	17.0
	1340	26.1	1295	0.0	+10.5	10.5
Double-pass 14 m	1305	42.3	1300	-40.6	-19.0	21.6
	1305	40.8	1300	-30.1	-9.7	20.4
	1305	40.5	1300	-20.5	-0.3	20.2
	1320	38.0	1300	-10.6	+6.0	16.6
	1330	31.9	1290	-0.5	+9.4	9.9